Expression and function of osteopontin variants in

HCV-related liver disease and hepatocellular carcinoma

Renée Jade Phillips, B. Biotech (Hons)

THE DEPARTMENT OF MICROBIOLOGY AND IMMUNOLOGY

THE SCHOOL OF MOLECULAR AND BIOMEDICAL SCIENCE

THE UNIVERSITY OF ADELAIDE

A dissertation submitted to The University of Adelaide

In candidature for the degree of

Doctor of Philosophy in the Faculty of Science

April 2010

CHAPTER 4: OPN and its role in cellular proliferation of HCC cell lines *in vitro*

4.1 Introduction

OPN is expressed in a wide range of cell types (see Section 1.3.3) and although readily secreted into the extracellular matrix, blood and urine, intracellular accumulation of OPN has also been described, particularly in cancer. Cellular OPN is particularly evident by immunohistochemistry (IHC) in tumorigenic hepatocytes at the leading edge of the tumor nodule, often adjacent to stromal cells (Gotoh et al., 2002); this has been shown in this thesis (Figure 3.1). This suggests that OPN may play a role at the intracellular level to modulate tumor cell proliferation, or alternatively secreted OPN from these cells may act locally in an autocrine or paracrine manner. Increased expression of OPN correlates with metastatic potential of HCC (Ye et al., 2003; Takafuji et al., 2007), however to date the role of OPN in cellular proliferation in HCC has not been well documented.

The numerous and varied functions of full-length OPN (OPN-A) have been well described, and range from normal physiological functions such as inflammation, immunity and bone remodelling, to those involved in carcinogenesis including tumor angiogenesis and metastasis (see Section 1.3.6), however little is known regarding the functions of variants OPN-B and OPN-C. The role of OPN in tumor cell proliferation is controversial, with OPN reported to increase the proliferation of prostate (Elgavish et al., 1998; Angelucci et al., 2004), head and neck squamous cell (Celetti et al., 2005), colon (Irby et al., 2004) and murine melanoma (Philip et al., 2001) cancer cells. Conversely, OPN was found to have no effect on the proliferation of breast cancer cell lines (He et al., 2006) or the HCC cell line HepG2 (Gao et al., 2003), and thus the role of OPN in proliferation is controversial and may be cell-type specific. All studies mentioned

82

above investigated the role of OPN-A in the proliferation process and thus the role of OPN and its variants in HCC remains to be defined.

Having earlier determined that OPN is expressed as three variants in HCC and HCV-related liver disease, this chapter **aims to investigate the expression and secretion of the three OPN variants (OPN-A, -B and –C) through the generation of expression vectors and over-expressing cell lines, and to evaluate their effect on HCC derived cell line proliferation and mechanisms through which this may occur.**

4.2   Results

4.2.1   Generation of OPN variant expression vectors

Expression plasmids for each of the three OPN variants (as described in Chapter 3) were constructed for transfection into cultured cell lines. Three OPN sequences of differing lengths representing OPN-A, -B and -C were amplified from a normal human liver cDNA library using primers OPN-F2 and OPN-R3 (see Table 2.1); sequencing confirmed that these three sequences represented OPN-A, -B and -C. Each variant was ligated into the mammalian expression vector pRc/CMV using *Xba*I and *Hind*III cloning sites. The success of the cloning procedure was confirmed by restriction digest of constructs with *Xba*I and *Hind*III, with visualisation of correct insert size by agarose gel electrophoresis (Figure 4.1) and automated sequencing of the excised bands to confirm the inserted sequence (data not shown).

4.2.2   Confirmation of OPN expression following transient transfection of OPN variant vectors

Each OPN variant expression vector was transiently transfected into naïve Huh-7 cells using FuGENE-6 Transfection Reagent. To confirm mRNA expression from each vector construct,
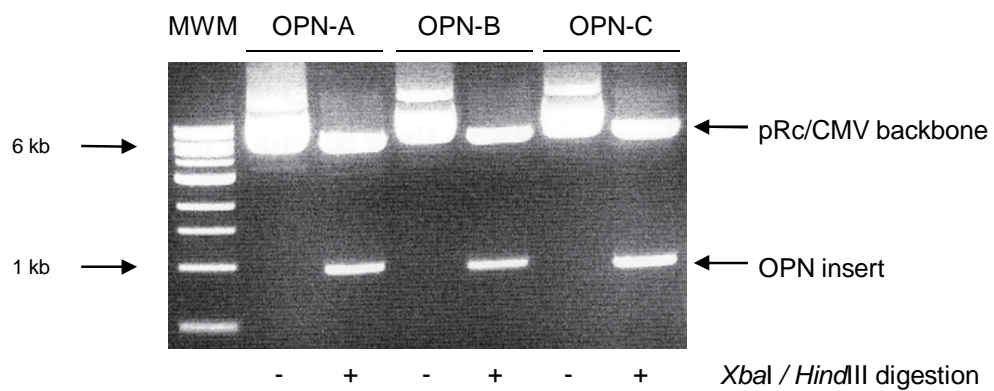
Figure 4.1 Agarose gel electrophoresis confirming successful cloning of the three OPN transcript variants into pRc/CMV. OPN vector constructs were digested with *Xba*I and *Hind*III (right lane) and run against uncut vector (left lane) to visualise bands representing the OPN variant inserts. Restriction enzyme digestion liberated bands of correct size for all three OPN vectors from the pRc/CMV vector backbone. MWM = 1 kb molecular weight marker.

total cellular RNA was harvested 72 hours post transfection using Trizol® Reagent. Following extensive DNase I treatment to remove input OPN cDNA, cDNA was prepared and subjected to RT-PCR using primers designed to amplify the three OPN variants concurrently (OPN-F2 and OPN-R3; see Table 2.1). Naïve and mock transfectant Huh-7s showed low level expression of each variant (Figure 4.2), which represents the basal level of OPN expression in Huh-7 cells. Huh-7 cells transfected with each OPN variant showed greatly increased expression of their corresponding variant.

To assess OPN variant protein production in transiently transfected cells, transfected Huh-7 monolayers were lysed directly in RIPA buffer (see Appendix 1) 72 hours post-transfection and total cellular protein lysates harvested and analysed by western blotting using an α-OPN antibody (K-20, Santa Cruz Biotechnology). Numerous attempts were made to visualise OPN protein by western blot, however specific OPN products of expected size could not be obtained (data not shown). The reasons for this could be numerous but may reflect the highly secreted nature of OPN resulting in undetectable levels of OPN within the transfected cells, or alternatively a low level of transfection efficiency resulting in insufficient OPN protein production for detection by western blotting.

4.2.3   OPN ELISA for detection of secreted OPN

4.2.3.1   Optimisation of in-house OPN ELISA

The negative attempt at detection of OPN by immunoblotting and the highly secreted nature of OPN prompted us to develop an in-house OPN ELISA for detection of secreted OPN in cell culture supernatant and patient serum samples. The optimal concentrations of capture and detection antibody were determined by testing combinations of capture antibody (α-OPN [MAB14331], R&D Systems) concentrations of 1 - 3 μg/ml with detection antibody (biotinylated
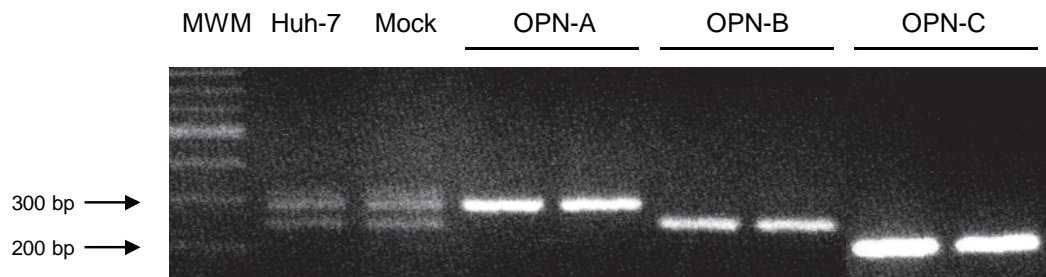
Figure 4.2 OPN PCR confirming over-expression of OPN-A, OPN-B and OPN-C transcripts in Huh-7 cells transiently transfected with each of the three variants, compared to naïve Huh-7 cells and Huh-7 cells transfected with empty pRc/CMV (Mock). MWM = 100 bp molecular weight marker.

α-OPN [BAF1433], RnD Systems) concentrations of 200 - 400 ng/ml in a number of pilot experiments. Serial 1/2 dilutions of recombinant human OPN protein (1433-OP, R&D Systems) were used in all experiments to generate a standard of known OPN concentrations, from which the OPN concentration of test samples could be calculated.

An initial test using high levels of recombinant human OPN standard (31.25 - 500 ng/ml) showed that a combination of 3 μg/ml capture antibody with either 200 ng/ml or 400 ng/ml detection antibody gave optimal absorbance results (Figure 4.3a). We therefore decided to use 200 ng/ml detection antibody for future experiments to minimise the amount of antibody required. This combination was tested in a second pilot experiment against an OPN standard curve of lower concentrations (7.81 - 125 ng/ml) to ensure that the assay could detect low levels of OPN in test samples. This test showed that the optimised assay could positively detect OPN at concentrations as low as 7.81 ng/ml (Figure 4.3b). Further optimisation of this assay for use with human serum and cell culture supernatant samples determined that, for optimal OPN detection, human serum samples should be diluted 1/3 and 1/5 and cell culture supernatants 1/2 and 1/3 for use in OPN ELISA (data not shown). This ELISA method was also tested for its ability to detect OPN in human urine, with results showing an average concentration of 1600 ng/ml in urine from healthy individuals when used at 1/10 dilution (n = 65; data not shown).

4.2.3.2 Confirmation of OPN secretion following transient transfection of OPN variant vectors

To confirm secretion of each of the three OPN variants from transiently transfected Huh-7 cells, OPN conditioned media was harvested, diluted in PBS and subjected to in-house sandwich OPN ELISA (as described above) to determine the concentration of secreted OPN in each sample.
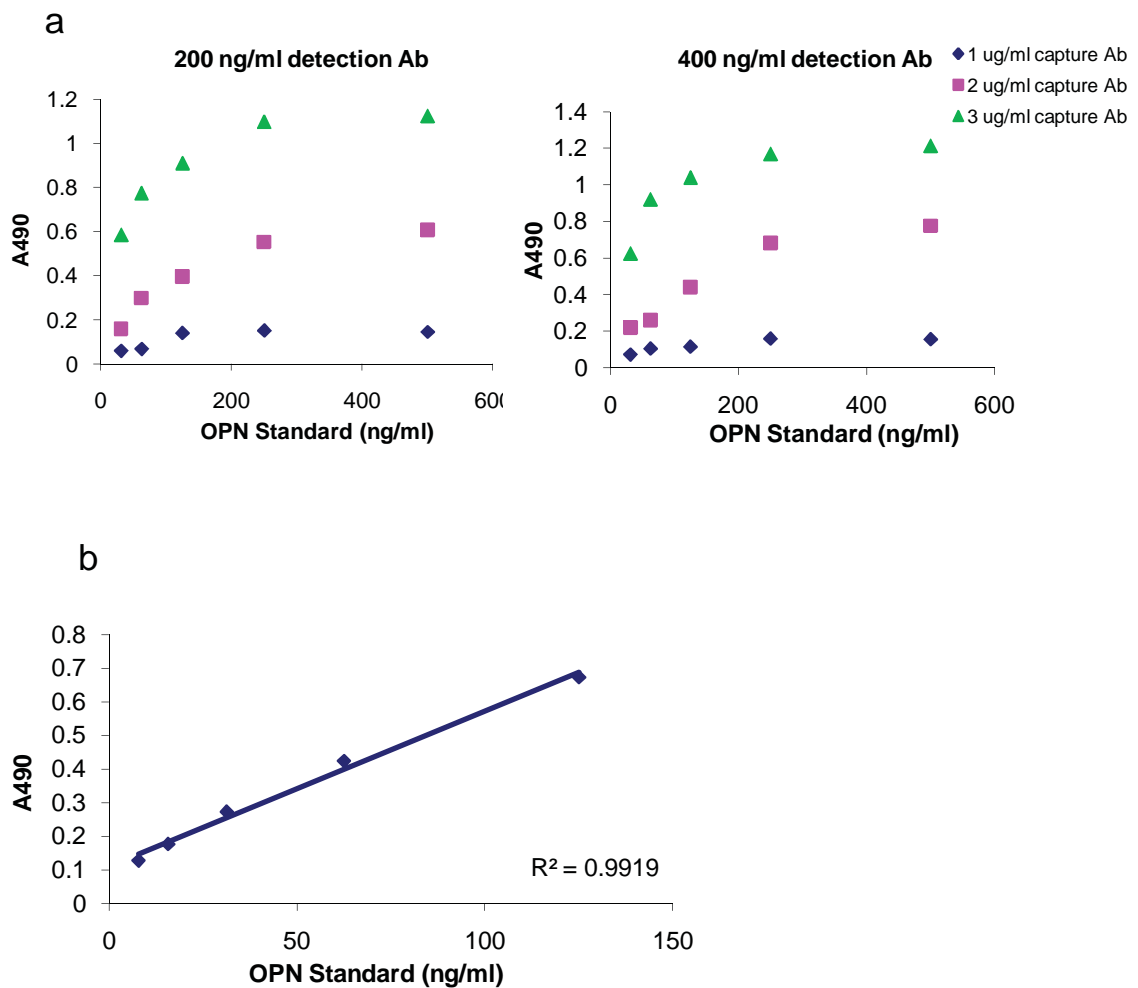
a

200 ng/ml detection Ab

400 ng/ml detection Ab

◆ 1 ug/ml capture Ab
■ 2 ug/ml capture Ab
▲ 3 ug/ml capture Ab

b

R² = 0.9919

Figure 4.3 In-house OPN ELISA optimisation. A pilot experiment (**a**) determined that the optimal concentrations for capture and detection antibody were 3 µg/ml and 200 or 400 ng/ml. 200 ng/ml detection was chosen for further experiments to minimise antibody requirements. A second pilot experiment (**b**) confirmed that the optimised ELISA conditions of 3 µg/ml capture antibody and 200 ng/ml detection antibody could detect recombinant human OPN as low as 7.81 ng/ml.

Media from OPN-A and OPN-B transfected Huh-7 cells possessed quantifiable concentrations of secreted OPN of 240.4 and 127.1 ng/ml respectively (Table 4.1).

	OPN (ng/ml)
Huh-7	n.d.
pRc/CMV	n.d.
OPN-A	240.4
OPN-B	127.1
OPN-C	n.d.

Table 4.1 Secreted OPN levels in cultured media from naïve Huh-7 cells, and Huh-7 cells transiently transfected with empty pRc/CMV or OPN variant vector

Secretion of OPN from both naïve and mock transfected Huh-7s was deemed to be below the detection limit of this assay (not detected; n.d.), although low levels of endogenous OPN may be present given that both cell lines are positive for OPN mRNA. OPN was not detected in samples from Huh-7s transfected with OPN-C, indicating one of three possibilities: OPN-C is not secreted, OPN-C is not detected by the antibodies used in this ELISA assay, or the levels of secretion are below the detection limits of the assay. Given that mRNA levels in transiently transfected cells are similar for all three variants (Figure 4.2), the confirmed secretion of OPN-A and OPN-B and the positive immunofluorescence staining for OPN-C (see Section 4.2.4 below), it can be logically assumed that OPN-C is secreted but not detected by the commercial detection antibody used in this ELISA assay. Information regarding epitopes used to generate the OPN antibodies used in this assay is not available.

4.2.4 Intracellular detection of OPN splice variants

OPN expression in HCC tissue reveals a cytoplasmic localisation pattern in addition to the highly secreted nature of OPN (Gotoh et al., 2002). This secreted function of OPN makes visualisation

difficult *in situ*, and as such there have been few if any reports on the cellular localisation of OPN in cultured cells. We hypothesise that the different OPN variants may have different sub-cellular localisations and in turn differing phenotypic effects. Expression patterns of the three OPN variants were investigated through the use of fluorescently-labeled antibodies and fluorescence microscopy.

Huh-7 cells were seeded onto glass coverslips and transiently transfected with expression vectors for each of the three OPN variants. To monitor transfection efficiency, Huh-7 cells were also transfected with pRc/CMV-e-GFP (containing a sequence for green fluorescent protein, see Section 2.1.1). 48 hours post-transfection, OPN-transfected cells were fixed in 1:1 acetone: methanol and stained with antibodies for OPN (K-20, Santa Cruz Biotechnology) and DAPI (Sigma). OPN was not detected in naïve Huh-7 cells, suggesting that endogenous OPN expression is well below the detection limits of the antibodies used, or alternatively that it is efficiently secreted (Figure 4.4). Visualisation of OPN-A, -B and –C transfected cells revealed that approximately 5% of cells expressed intracellular OPN, in contrast to e-GFP transfected cells which showed positive expression in 40 - 50% of cells (data not shown). Assuming that transfection efficiency is similar for all Huh-7 cells, this result suggests that the majority of OPN is efficiently secreted as expected. In cells expressing OPN, each variant had a slightly different sub-cellular localisation. OPN-A revealed a diffuse cytoplasmic localisation while OPN-B showed a punctuate pattern and OPN-C revealed a more globular arrangement. These pilot experiments suggest that OPN variants when localised to the cytosol may have different effects on cell homeostasis. They also confirm the protein expression of OPN-C in the absence of a positive ELISA (see above). These observations suggest further experiments are warranted but are beyond the scope of this thesis.
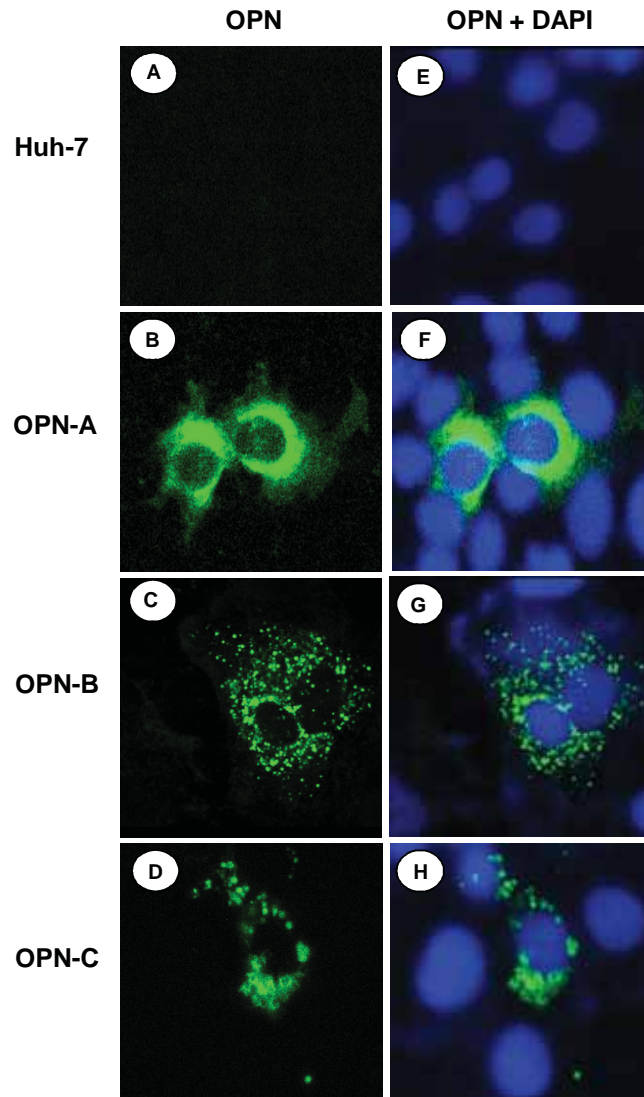
Figure 4.4 Immunofluorescent staining of OPN in Huh-7 cells transiently transfected with OPN-A, OPN-B and OPN-C-expressing vectors (K-20 α-OPN). OPN expression in naïve Huh-7 cells is below the level of detection for this assay **(A)**. Over-expression of the three OPN variants showed exclusively cytoplasmic staining but in differing patterns: diffuse for OPN-A **(B)**, punctate for OPN-B **(C)**, and globular for OPN-C **(D)**. Cells were counterstained with DAPI to visualise nuclear DNA **(E-H)**. All pictures were taken at 20× lens magnification.

4.2.5 Generation of OPN stable transfectant Huh-7 cell lines

In order to perform studies examining the role of the OPN variants in cellular proliferation, it was necessary to derive stable cell lines expressing each of the variants. This would alleviate any issues associated with transient transfection studies such as inconsistent transfection efficiencies. It was decided to construct stable cell lines in Huh-7 cells, as endogenous expression of OPN mRNA in these Huh-7 cells is low, as reported by us (Section 3.2.1) and others (Kim, H. J. et al., 2009), and secretion undetectable by ELISA (Section 4.2.3.2).

To generate constitutively expressing OPN variant Huh-7 clonal populations, Huh-7 cell monolayers were transfected with either OPN variant vectors (OPN-A, -B or –C) or mock transfected with empty vector (pRc/CMV). Selection for transfected cells was performed by the addition of 500 μg/ml G418 sulphate to the cell culture media. Cells were sub-cultured at low density to allow for single colony expansion. 15 clones for each OPN variant were selected by colony ring harvest and assessed for secretion of OPN into culture media by in-house sandwich OPN ELISA. Secreted OPN was not detected in conditioned media from untransfected parental or vector only transfected Huh-7 cells (data not shown). Three clones each for OPN-A and OPN-B were deemed positive for OPN secretion into culture media (Figure 4.5); these (A8, A12, A14 and B4, B12, B14) and three "negative" (A3, A7, A13 and B1, B3, B13) clones for each variant were expanded and stored. OPN was not detected in any OPN-C clone, three of which (C3, C4, C5) were stored as "negative" stable cell lines. A second set of 22 transfected clones for OPN-C were generated, with no secreted OPN detected for any line (data not shown). The lack of detection of OPN secretion in OPN-C stable cell lines is consistent with data from transiently transfected Huh-7 cells described previously (Section 4.2.3.2).
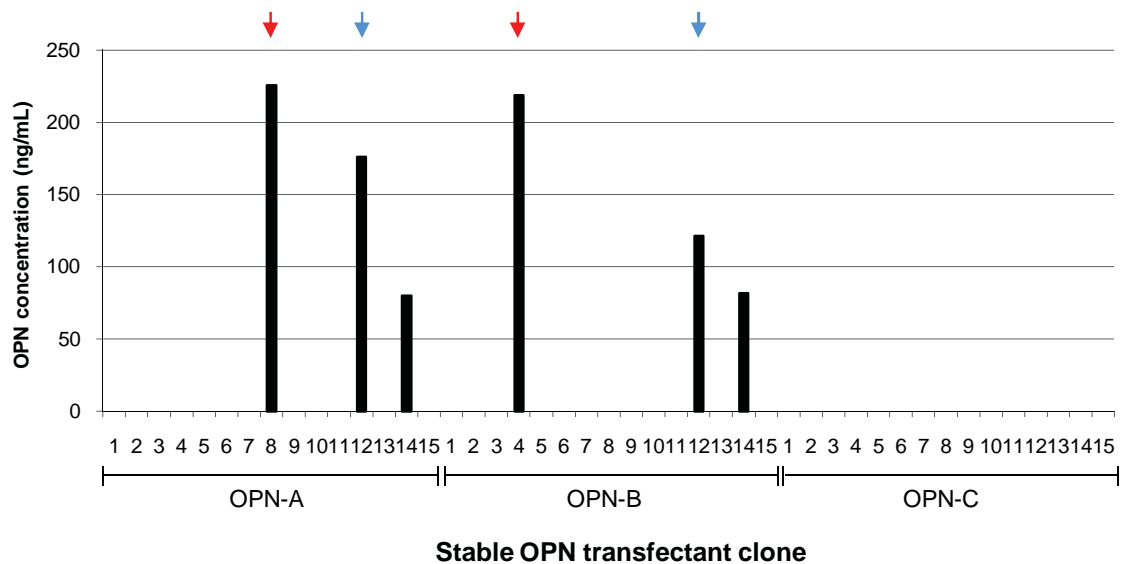
Figure 4.5 OPN ELISA confirming secretion of OPN-A and OPN-B protein from stably transfected cell lines. Untransfected and mock pRc/CMV transfected Huh-7 cells tested negative for secreted OPN against a standard curve of recombinant human OPN (data not shown). Three clones each of OPN-A (A8, A12 and A14) and OPN-B (B4, B12 and B14) transfectants tested positive for secreted OPN. Red arrows indicate the highest OPN expressing clones, which were chosen for further analysis. Blue arrows indicate the second highest OPN expressing clones, which were chosen for further analysis as a clonal alternative. Detection of secreted OPN from OPN-C transfectants was not evident in this assay, as discussed in Section 4.2.3.2.

OPN mRNA was confirmed by RT-PCR; all positive OPN-A (Figure 4.6 top) and OPN-B (Figure 4.6 middle) clones (as determined by OPN ELISA) showed positive expression of the corresponding OPN variant, whilst all negative clones showed weak expression of all three OPN variants in a similar pattern to that seen previously in this thesis for naïve Huh-7 cells (data not shown). The entire second set of OPN-C clones generated was also tested for OPN mRNA expression; 11 of 22 clones tested positive for OPN-C mRNA only (example shown in Figure 4.6 bottom). These OPN-C over-expressors were now deemed "positive" clones, three of which (C1, C2, C11) were expanded and stored for further experiments.

Detection of OPN protein expression in stably transfected cells was attempted by *in situ* detection and western blotting. OPN was not visualised in any of the positive or negative stable transfectants by immunofluoresence (data not shown), however bands of varying sizes (representing the three variants) were visualised in cellular lysates from positive clones of each variant as detected by western blotting (Figure 4.7a). Detection of secreted OPN by western blotting was also attempted using conditioned media from stably transfected cells that was concentrated to one fifth of its original volume to enhance OPN detection. Strong OPN expression was noted for both OPN-A and –B (Figure 4.7b) of similar size to cellular protein seen in Figure 4.7a, however signal for secreted OPN-C was very weak and of larger size than cellular protein, suggesting that OPN-C may undergo post-translational modifications prior to secretion. These results outline the successful construction of stable cell lines expressing each of the OPN transcript variants, as confirmed by expression of OPN splice variant mRNA and secretion of OPN protein as detected by ELISA and western blotting.

4.2.6 Effect of OPN on HCC-derived cell line proliferation

Uncontrolled cellular growth and division is a hallmark of cancer progression. This is often controlled by the increased expression of growth factors and the mutation of genes involved in
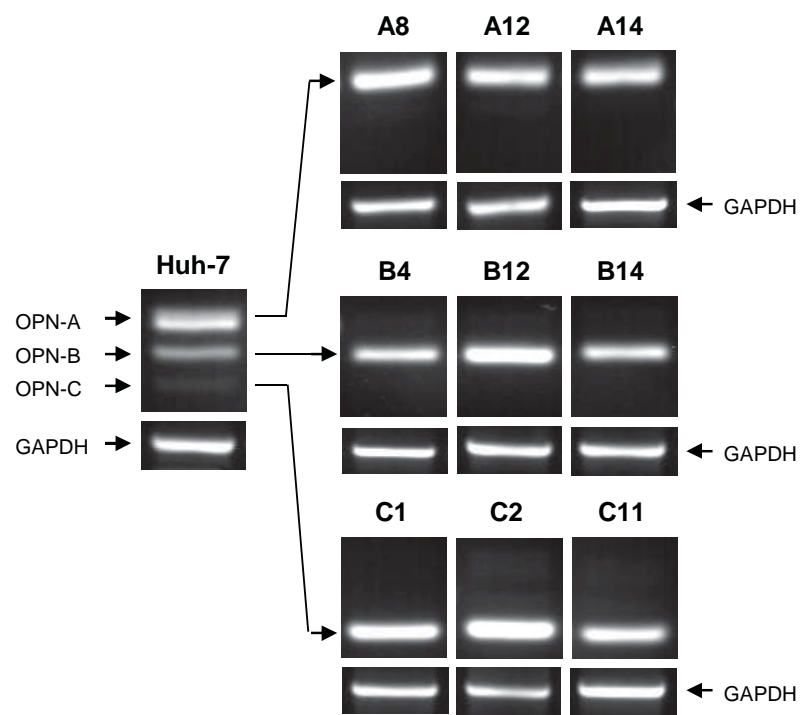
Figure 4.6 OPN RT-PCR confirming mRNA expression of each OPN variant in stably transfected clones.
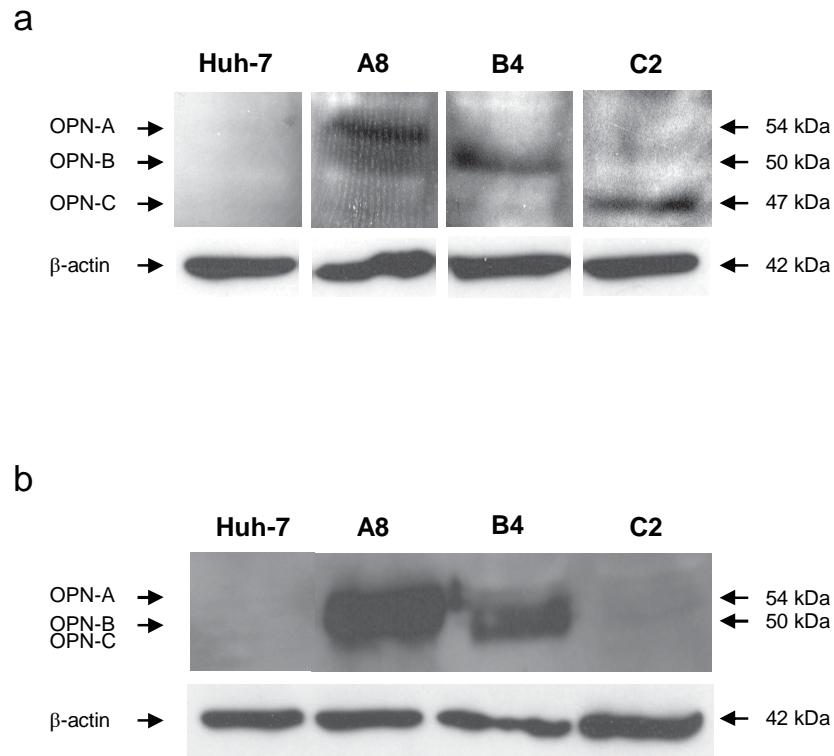
Figure 4.7 Western blot confirming cellular expression **(A)** and secretion **(B)** of all three OPN variants in stably transfected cell lines. Expression of OPN from naïve Huh-7 cells is below the detection limit of the assay. Stable transfectants of each of the OPN splice variants shows strong cellular protein expression of their corresponding variant, whilst both OPN-A and –B showed strong OPN secretion. OPN-C showed very weak levels of secreted protein but at a larger size than cellular protein, suggesting post-translational modifications may occur for this variant.

cell cycle arrest, therefore allowing the cell cycle to proceed unchecked. The role of OPN in the proliferation of tumor cells remains a controversial subject. This study aimed to investigate the effect of OPN expression on the rate of cellular growth of hepatoma cells, and to identify potential cellular mechanisms through which OPN may be exerting this effect (if any). An average 30% increase in *in vitro* cellular proliferation has been shown in four colon cancer cell lines (HCT 116, HT29, KMC12 and SW480) stably over-expressing OPN compared to mock transfected cells (Irby et al., 2004). OPN has also been shown to increase proliferation of both cultured prostate epithelial cells (Elgavish et al., 1998) and prostate carcinoma (LNCaP) (Angelucci et al., 2004) and murine melanoma (B16F10) (Philip et al., 2001) cell lines, both *in vitro* and *in vivo*. Increased proliferation of HSCs following incubation with OPN has also been demonstrated (Lee, S. H. et al., 2004), suggesting a role for OPN in accelerating growth of cells in the liver, however the effect of OPN on proliferation of tumorigenic hepatocytes has been relatively unexplored, although a recent study utilising lentiviral-mediated RNA knockdown of OPN suggested a role for OPN in the proliferation of a hepatoma-derived cell line (HCCLM3) both *in vitro* and in an *in vivo* murine tumor growth model (Sun, B. S. et al., 2008). The wide range of studies indicating a role for OPN in cancer cell proliferation in a number of tumor types suggests that this phenomenon may occur in hepatoma cells, although the role of the alternatively spliced variants OPN-B and OPN-C has not been explored.

4.2.6.1 Effect of intracellular OPN expression on hepatoma cell proliferation

To investigate the effect of OPN expression on the growth of human hepatoma cells, the proliferation of clonal Huh-7 cells stably expressing each of the three OPN variants was monitored over a 4 day period. Clones with the highest level of OPN secretion were initially selected (namely A8 for OPN-A [225.5 ng/ml], B4 for OPN-B [218.8 ng/ml]; see Figure 4.5). As secreted OPN could not be quantitated from OPN-C stable clones by ELISA, clone C2 was chosen for OPN-C as it had the strongest band intensity during OPN RT-PCR (Figure 4.6) and

expressed OPN protein as detected by western blotting (Figure 4.7). The chosen clones were plated at identical cell densities, with trypan blue exclusion cell counts performed every 24 hours over a 4 day period. Parental and mock transfected (i.e. cells transfected with empty pRc/CMV) Huh-7 cells were counted concurrently to act as baseline growth controls. No difference in cell number was observed over 4 days between the two control cell lines (Figure 4.8 black dashed lines). A significant increase in cell number was noted at days 3 and 4 post-seeding for all OPN expressing clones compared to controls (Figure 4.8 coloured lines, $p < 0.05$). This experiment was repeated with another clone for each variant (namely A12, B12 and C1). A similar significant increase in cellular growth at days 3 and 4 above the control cell lines was observed for all clones ($p < 0.05$, data not shown), indicating that this increase was not due to clonal selection bias.

4.2.6.2 Secreted OPN increases proliferation of naïve hepatoma cells

The results obtained above suggest that expression of all three OPN variants can promote increased Huh-7 cellular proliferation, however this does not indicate whether the observed effect is due to an intracellular effect or an autocrine or paracrine effect of secreted OPN given that OPN is efficiently secreted. We hypothesise that secreted OPN could act in an autocrine or paracrine manner to promote cellular proliferation. To test this hypothesis, conditioned media was prepared from OPN variant clones (A8, B4 and C2). Naïve Huh-7 cells were seeded in OPN variant conditioned media and monitored every 24 hours for 4 days. Huh-7 cells were also seeded in conditioned media from parental and mock transfected Huh-7 cells as controls with no difference in proliferation observed (Figure 4.9 black dashed lines). Significantly higher cell numbers were seen for Huh-7 cells grown in OPN conditioned media from all three variants compared to controls at days 3 and 4 post-seeding (Figure 4.9 coloured lines, $p < 0.05$), indicating that secreted OPN variants can increase the proliferation of Huh-7 cells in a paracrine
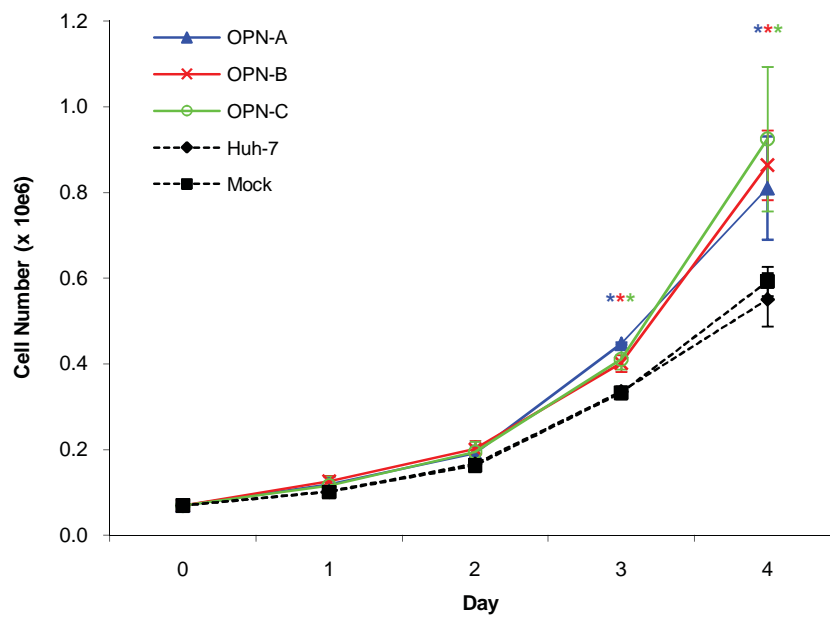
Figure 4.8 Intracellular expression of each of the OPN variants results in increased cellular proliferation. No significant difference between growth of Huh-7 cells and a mock transfectant cell line was observed. However, all variant stable cell lines showed significantly greater growth than both control cell lines at days 3 and 4 post seeding. A repeat experiment using a second clonal cell line for each OPN variant showed similar increases in cellular proliferation (data not shown). * $p < 0.05$.
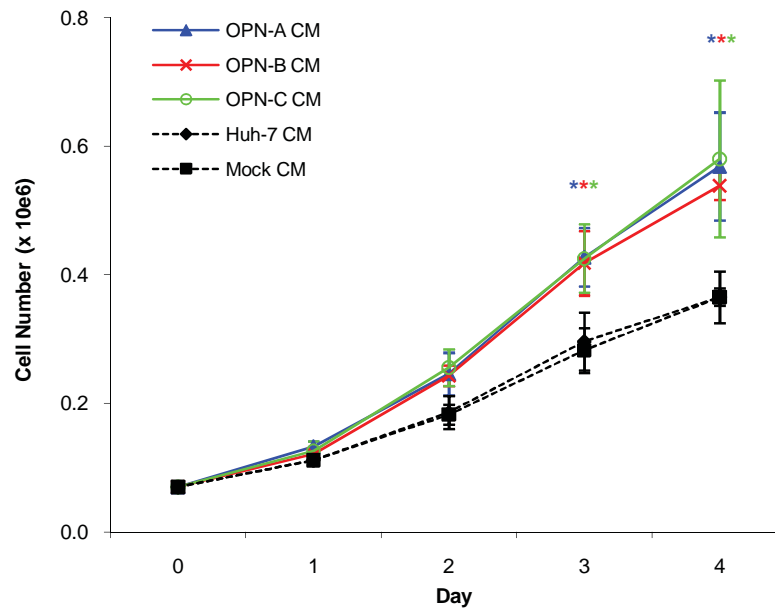
Figure 4.9 Secretion of all OPN variants amplifies the cellular growth rate of naïve Huh-7 cells. Huh-7 cells were seeded in conditioned media (CM) from OPN stably transfected cell lines, and naïve and mock transfected Huh-7 cells as controls. No significant difference in cell number was observed between controls. However, Huh-7 cells grown in cultured media from all OPN variant cell lines show significantly greater growth than both controls at days 3 and 4 post seeding. A repeat experiment using a second clonal cell line for each OPN variant showed similar increases in cellular proliferation (data not shown). CM = conditioned media. * $p < 0.05$.

manner. This experiment was repeated with a second highly over-expressing clone for each variant with similar results observed (A12, B12, and C1: $p < 0.05$, data not shown).

To investigate whether the paracrine effect of OPN variants on cellular proliferation is a cell line-specific observation, the above experiment was repeated on another human hepatoma cell line. HepG2 cells were seeded in an identical manner to naïve Huh-7 cells in conditioned media prepared from stably transfected OPN variant clones (as outlined above) and parental and mock transfected Huh-7s. Over a 4 day growth period, significantly increased cell numbers were observed at days 3 and 4 of growth for HepG2 cells grown in conditioned media from all three OPN stable clones compared to both controls (Figure 4.10, $p < 0.05$). This effect was also observed in HepG2 cells grown in conditioned media from a second set of OPN stable clones as outlined above ($p < 0.05$, data not shown).

4.2.6.3   Blocking cell surface binding of OPN abrogates hepatoma cell proliferation

The above results suggest an OPN effect on cellular proliferation. To confirm this, an OPN-blocking antibody was used to prevent OPN binding to cell surface receptors. This antibody binds near the C terminus of OPN which is also the location of the OPN CD44 binding motif (Santa Cruz Biotechnology). Huh-7 cells were seeded in cultured media from both naïve Huh-7 and OPN-A stably transfected (A8) cells. Three sets of cells were plated; one in conditioned media alone, a second in conditioned media with the addition of an anti-OPN blocking antibody (K-20, Santa Cruz Biotechnology), and a third in conditioned media with the addition of an antibody isotype control (unrelated rabbit IgG, Santa Cruz Biotechnology). This control antibody was used to negate any effect observed simply from the addition of an antibody to the conditioned media.
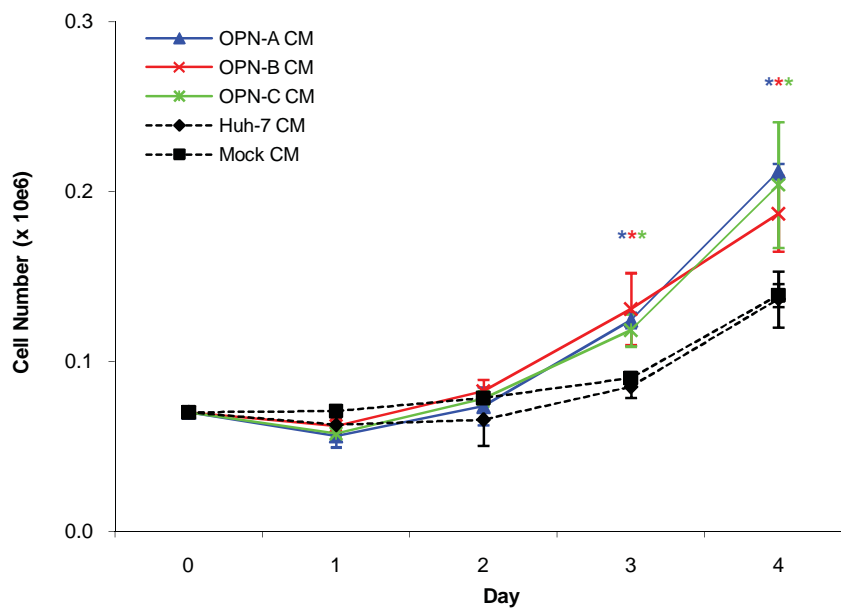
Figure 4.10 Secretion of all OPN variants amplifies the cellular growth rate of HepG2 cells at days 3 and 4 post seeding in a similar manner to Huh-7 cells, suggesting that OPN-mediated acceleration of hepatoma cell proliferation is not cell-line specific. Experiments were performed as previously described for Huh-7 cells (Figure 4.9). A repeat experiment using a second clonal cell line for each OPN variant showed similar increases in cellular proliferation (data not shown). CM = conditioned media. * $p < 0.05$.

No difference in cell number was observed for Huh-7 cells grown in Huh-7 conditioned media irrespective of the presence or absence of either antibody (Figure 4.11 black dashed lines), suggesting that low levels of endogenously produced OPN-A do not contribute to increased Huh-7 proliferation. Naïve Huh-7 cells grown in OPN-A conditioned media alone (blue) and in the presence of redundant antibody (purple) both showed significantly increased cell number on days 3 and 4 of growth (both $p < 0.05$), however the addition of an anti-OPN antibody (orange) resulted in no observable increase in proliferation over the controls. This experiment was repeated with conditioned media from a second OPN-A clone (A12) with similar results ($p < 0.05$, data not shown). These results indicate that cellular proliferation of cultured hepatoma cells is increased in a paracrine manner in the presence of all three OPN variants.

4.2.7 Effect of OPN-CD44 interaction on hepatoma cell proliferation

CD44 is one of two cell surface receptors for OPN, the other being the integrins. It was first isolated in haemopoietic cells (Jalkanen et al., 1986), and sequences have been identified in a wide range of species. CD44 undergoes extensive splicing giving rise to a large number of isoforms, incorporating differing arrangements of the 9 variant (v) exons between the 10 constant exons. The standard form of human CD44 (CD44s) contains all 10 constant exons but no variant exons, and is therefore the smallest isoform. CD44s is ubiquitously expressed throughout the body, whereas isoforms containing one or more variant exons are typically expressed in proliferating cells within some epithelial tissues, and in a number of cancers (Ponta et al., 2003). CD44 expression has been noted in a wide variety of carcinoma cell lines, including those from melanoma and colon cancer, and in many solid tumors including mesothelioma, melanoma, oesophogeal cancer, colon adenocarcinoma and thyroid cancer (Stamenkovic et al., 1989).

The interaction between OPN and CD44 on the cell surface has been widely investigated. OPN specifically binds CD44 variant exons v6 or v7, and may also bind v3 via a heparin bridge
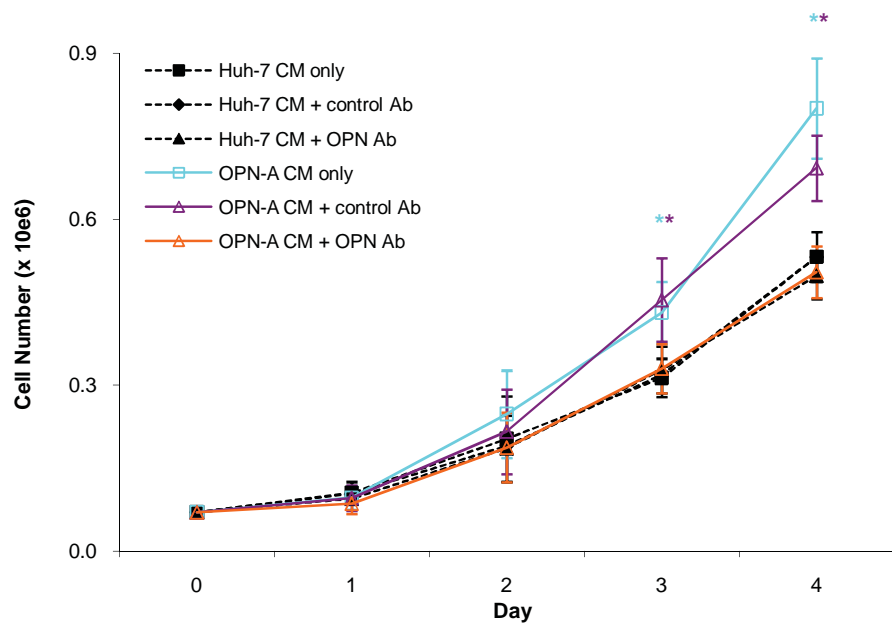
Figure 4.11 Addition of anti-OPN antibody to conditioned media (CM) from OPN-A expressing cells blocks the paracrine effect of secreted OPN on cellular growth of Huh-7 cells. Huh-7 cells with OPN-A cultured media alone and with an isotype control antibody showed increased growth over baseline controls, however addition of anti-OPN antibody abrogated this increased growth. The addition of isotype control or anti-OPN antibodies to Huh-7 cultured media did not affect the growth of Huh-7 cells. * $p < 0.05$.

(Weber et al., 1996; Katagiri et al., 1999). This interaction is RGD-independent but requires the presence of β1 integrins (Katagiri et al., 1999). When interaction between OPN and CD44 v6/v7 occurs on the tumor cell surface, it induces transcription of CD44 and increased cell surface expression of CD44s, v6 and v9 (Khan et al., 2005). This interaction mediates chemotaxis and adhesion of T cells, fibroblasts, and bone marrow cells (Weber et al., 1996; Denhardt, Noda et al., 2001; Wai and Kuo 2004) and down-regulates IL-10 expression in peritoneal macrophages (Ashkar et al., 2000). The CD44-OPN interaction has also been suggested to promote proliferation and survival of IL-3-dependent bone marrow cells; secreted OPN has been shown to increase proliferation of a mouse pro B cell line, however this effect was blocked by the addition of either anti-OPN or anti-CD44 antibodies (Lin, Y. H. et al., 2000). Another recent study showed that OPN-induced increases in oral cavity squamous cell carcinoma proliferation can be abrogated by antibody blocking of CD44 (Celetti et al., 2005). These results indicate that the increased proliferative effect of OPN may be mediated through its interaction with CD44. This section of the thesis aims to investigate this effect in the context of human hepatoma cells in the hope of establishing a similar precedent for OPN in tumorigenic hepatocytes.

4.2.7.1   CD44 expression in carcinoma cell lines

In order to determine whether OPN exerts its increased proliferative effect through interactions with CD44, it was first imperative to determine if Huh-7 and HepG2 cells express CD44. We therefore investigated CD44 expression levels in both Huh-7 and HepG2, as well as HeLa (a known high CD44 expressing cell line) (Charnaux et al., 2005) and Hep3B (a CD44 negative cell line) (Cruickshank et al., 1998). CD44 mRNA expression was detected by RT-PCR using primers CD44s-F and CD44s-R (see Table 2.1) that bind within the constant exons of CD44 (and therefore simultaneously amplify all CD44 variants). The high-CD44 expressing cell line HeLa showed high levels of CD44 mRNA whilst Hep3B showed no expression as expected

(Figure 4.12a). Huh-7 cells expressed CD44 mRNA, whilst HepG2 showed low (but detectable) mRNA expression.

CD44 protein expression (or lack thereof) was confirmed by immunofluorescence microscopy. Each of the four cell lines was seeded onto glass coverslips in 24-well tissue culture plates and stained with an antibody to detect CD44 (NeoMarkers) and the nuclear marker DAPI (Sigma). Strong CD44 expression was noted for both Huh-7 and HeLa, while weak staining was noted for HepG2 and no staining noted for Hep3B (Figure 4.12b). These immunofluorescence experiments were performed on unpermeabilised cells and as such represent cell surface expression of CD44 and correlate with mRNA expression.

4.2.7.2 Effect of cellular CD44 status on OPN-induced increases in carcinoma cell proliferation

This chapter has already shown an increase in proliferation for two CD44$^+$ cell lines (Huh-7 and HepG2) when exposed to OPN conditioned media (Section 4.2.6.2). To extend these observations, we investigated the effect of OPN on the CD44$^-$ hepatoma cell line Hep3B and the CD44$^+$ cervical carcinoma cell line HeLa. Both cell lines were seeded in OPN conditioned media and their proliferation monitored every 24 hours for 4 days along with appropriate controls. The presence of each of the three OPN variants resulted in significantly higher cell number for HeLa cells at days 3 and 4 of growth (Figure 4.13a coloured lines, $p < 0.05$), but no change for the Hep3B cell line (Figure 4.13b coloured lines). Both cell lines were tested with conditioned media from a second set of clones with similar results ($p < 0.05$, data not shown). These results are suggestive (but not conclusive) of CD44 playing a role in OPN-induced cellular proliferation.

a

	Huh-7	HepG2	Hep3B	HeLa
CD44s				
GAPDH				

b
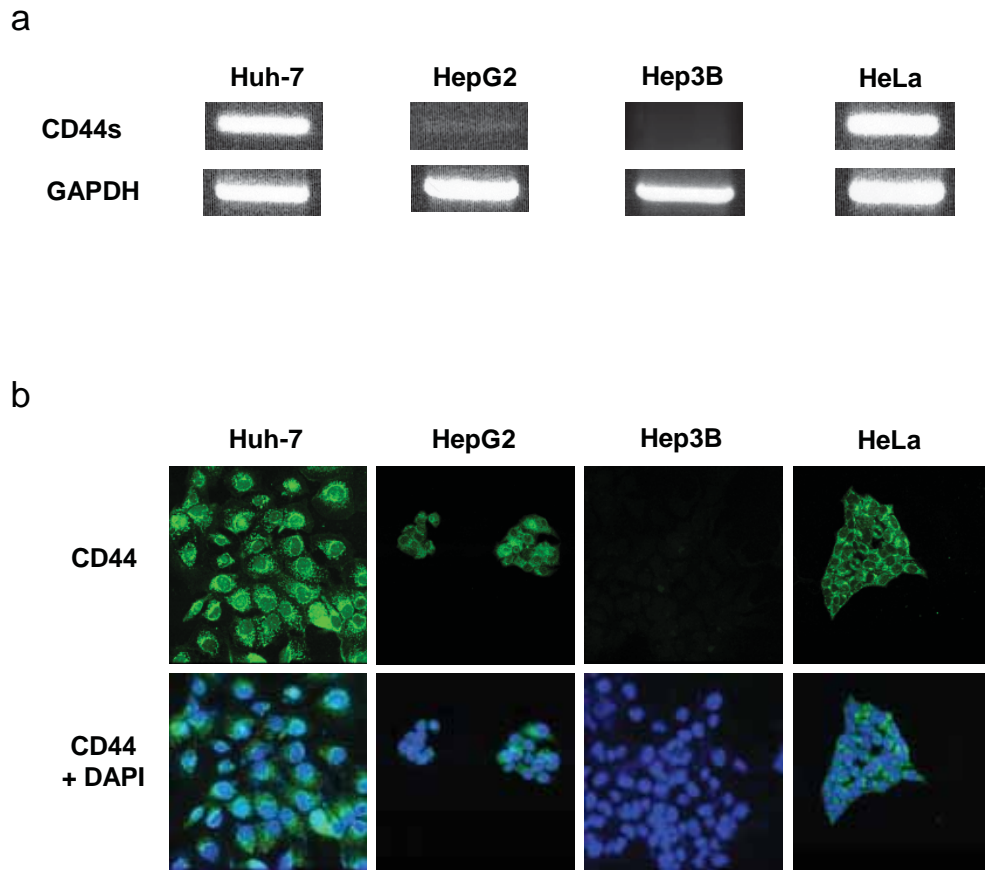
Figure 4.12 Huh-7, HepG2 and HeLa cultured cell lines express CD44 on the cell surface, but Hep3B cells do not. Top: RT-PCR for CD44s resulted in strong expression in Huh-7 and HeLa cells, weak expression in HepG2 cells and complete absence in Hep3B cells. The housekeeping gene GAPDH served as an internal loading control. Bottom: All cell lines were immunofluorescently stained for CD44 (NeoMarkers). Huh-7 and HeLa showed strong cell surface staining for CD44, HepG2 was weakly positive for CD44, and Hep3B was negative for CD44 as expected.
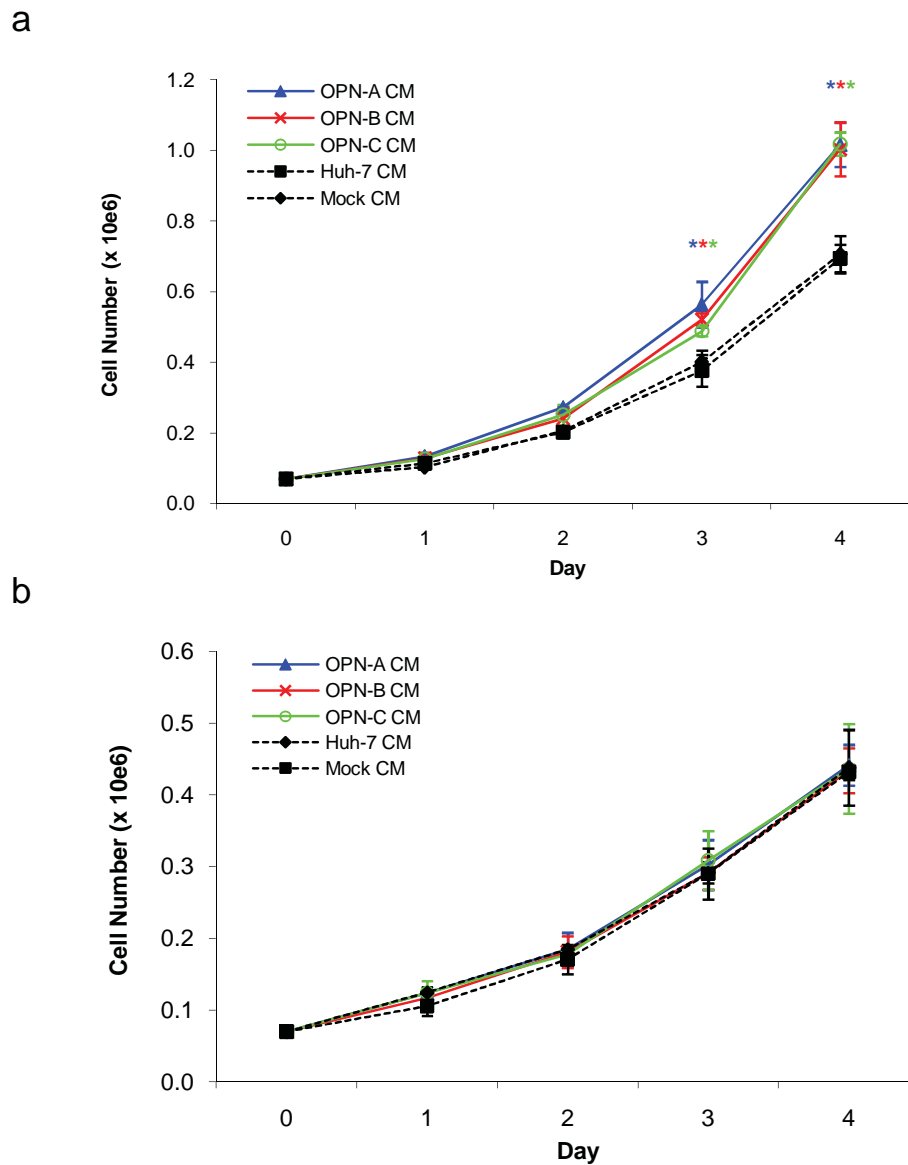
Figure 4.13 Secretion of all OPN variants amplifies cellular growth rate of **(a)** HeLa cells at days 3 and 4 post seeding but not **(b)** Hep3B, suggesting that OPN-mediated acceleration of hepatoma cell proliferation requires the presence of CD44. Experiments were performed as previously described for Huh-7 cells (Figure 4.9). A repeat experiment using a second clonal cell line for each OPN variant showed similar results (data not shown). CM = conditioned media. * $p < 0.05$

4.2.7.3 Effect of siRNA knockdown of CD44 on OPN-induced increases in cellular proliferation

To further investigate the requirement of CD44 in OPN-mediated acceleration of cellular proliferation *in vitro*, CD44 expression in cultured carcinoma cells was abrogated by short interfering RNA (siRNA) knockdown of all CD44 sequences. By silencing expression of CD44, we are in effect creating a CD44-null environment within which to investigate its role in OPN-mediated increases in cellular proliferation. siRNA sequences are short double-stranded RNA oligonucleotides first discovered in plants (Hamilton and Baulcombe 1999) that specifically inhibit mRNA expression of target genes via the RNA interference (RNAi) pathway (Figure 4.14). Synthetic siRNA oligos are introduced into cultured cells via lipid-based transfection and associate with an RNAse-containing complex to form the RNAi-induced silencing complex (RISC), which unwinds the siRNA double strand and releases the sense strand. The remaining anti-sense strand recognises and cleaves complimentary sequences within the cellular mRNA, resulting in mRNA degradation and silencing of the target gene. siRNAs are therefore an important research tool for investigating gene functions and interactions (Carthew and Sontheimer 2009).

4.2.7.4 Optimisation and validation of CD44 knockdown

Prior to siRNA knock-down of CD44, siRNA transfection efficiencies in the chosen cell lines were optimised to ensure efficient knock-down of CD44. Huh-7 and HeLa cells were seeded in 6-well tissue culture plates and transfected (using Lipofectamine 2000^{TM} [Invitrogen]) with 8 nM, 20 nM and 40 nM of BLOCK-iT^{TM} Fluorescent Oligo (Invitrogen), a fluorescein-labeled double-stranded RNA oligomer with the same length, charge and configuration as standard siRNA oligonucleotides. The BLOCK-iT^{TM} Fluorescent Oligo sequence localises to the cell nucleus, is not homologous to any known gene, and emits a strong fluorescent signal for up to
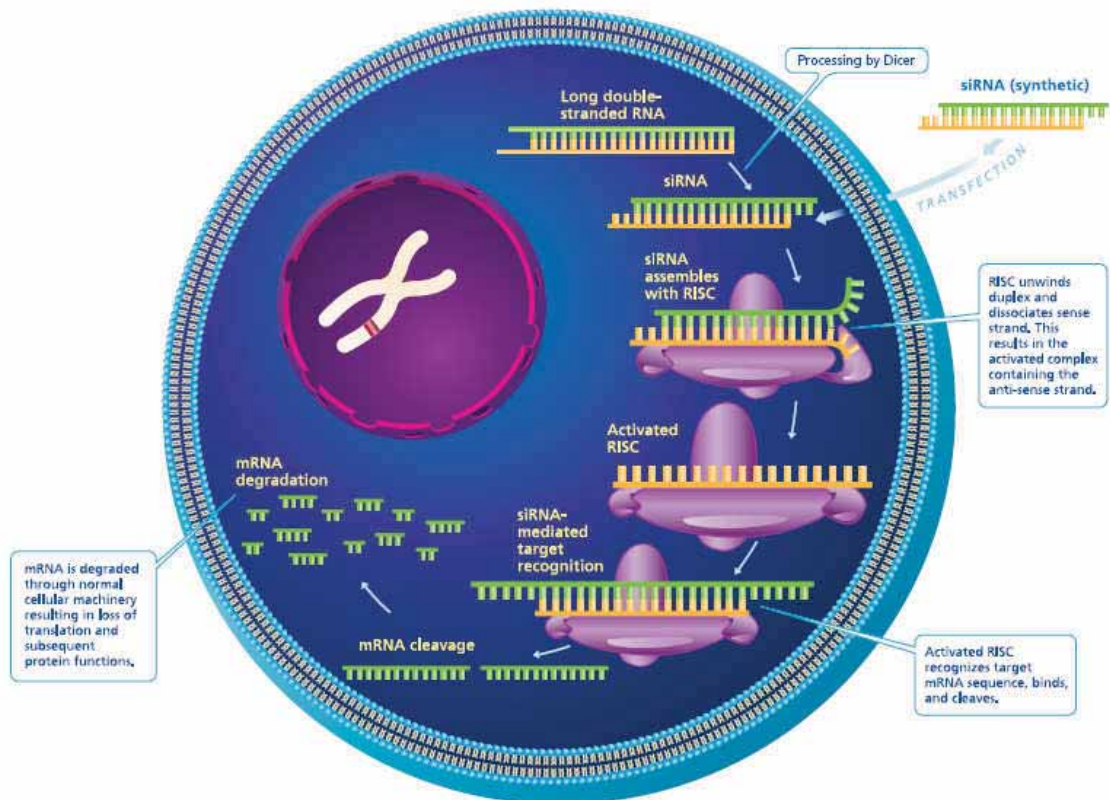
Figure 4.14 The RNAi interference pathway. Synthetic siRNA oligos are introduced into the cell via lipid-based transfection and associate with an RNAse-containing complex to form the RNAi-induced silencing complex (RISC), which unwinds the siRNA double strand and releases the sense strand. The remaining anti-sense strand recognises and cleaves complimentary sequences within the cellular mRNA, resulting in mRNA degradation and silencing of the target gene.

72 hours. It was used in this study to give an indication of the expected transfection efficiency of siRNA oligonucleotides in the chosen cell lines, as greater efficiency and targeting to all cells will result in a greater knockdown of CD44.

The percentage of cells successfully transfected with BLOCK-iT^{TM} Fluorescent Oligo was determined by visually counting viable FITC-positive cells in $10 \times$ magnification fields on a fluorescence microscope using a standard FITC filter set ($\lambda_{excitation} = 494$ nm; $\lambda_{emission} = 519$ nm). Both Huh-7 and HeLa cells transfected with 8 nM BLOCK-iT^{TM} showed less than 20% positive cells with very weak signal intensity (data not shown). However, both cell lines showed greater than 90% transfection efficiency when transfected with either 20 nM or 40 nM BLOCK-iT^{TM} (Figure 4.15). Huh-7 transfection efficiencies were comparable between 20 nM (97%) and 40 nM (96%), however transfection was slightly higher in HeLa cells at 40 nM (99%) than 20 nM (97%). Therefore, 40 nM was chosen as the optimal siRNA concentration with which to transfect both Huh-7 and HeLa cells for CD44 knock-down.

Three 25 bp blunt-ended Stealth^{TM} siRNA sequences (Invitrogen) for CD44 knockdown were received from Invitrogen:

1. CD44-HSS101596 (hereafter termed "siRNA 1")
2. CD44-HSS101597 (hereafter termed "siRNA 2")
3. CD44-HSS101598 (hereafter termed "siRNA 3")

Each sequence binds to complementary sequences within, or at junctions between, the constant exons of CD44, and is therefore able to minimise expression of all CD44 isoforms (Figure 4.16). The ability of each siRNA sequence to silence CD44 expression in both Huh-7 and HeLa cell lines was tested by analysis of CD44 mRNA using RT-PCR. Both cell lines were seeded in 6 well plates and transfected in duplicate wells with 40 nM of each of the three CD44 siRNA

sequences using Lipofectamine 2000^{TM} (Invitrogen). Duplicate wells of each cell line were also transfected with a scrambled control siRNA sequence provided by Invitrogen (Stealth RNAi Negative Control Med GC); this sequence does not bind to any known mRNA sequence and was used in this experiment to control for siRNA transfection and any other off-target effects that the siRNAs may have. Duplicate untransfected wells were used as an additional control to monitor native CD44 expression in both cell lines. Cell monolayers were transfected and RNA harvested from one duplicate well 24 hours and the other 48 hours post transfection. cDNA was prepared and CD44 expression levels monitored by RT-PCR using primers for CD44s (see Table 2.1). While only semi-quantitative, all three siRNA sequences showed clear knockdown of CD44 expression in Huh-7 cells at 24 and 48 hours post transfection (Figure 4.17 top), however in HeLa cells each of the siRNA sequences showed only slight knockdown at 24 hours post transfection which most likely reflects the high basal level of CD44 expression in these cells (Figure 4.17 bottom). In HeLa cells, siRNA 1 and siRNA 2 showed clear knockdown at 48 hours post transfection, whereas knockdown for siRNA 3 was not as efficient.

Decreases in CD44 protein levels were similarly examined in both cell lines to investigate whether the strong knockdown in mRNA expression correlated with a concurrent decrease in CD44 protein. Both cell lines were seeded and transfected in duplicate as described above with similar controls. Cellular protein was harvested from one duplicate well 24 hours and the other 48 hours post transfection. Protein lysates were electrophoresed on SDS-PAGE gels and CD44 protein detected by western blotting using an anti-CD44 antibody (CD44 Std/HCAM Ab-4, NeoMarkers). OPN specific bands could not be obtained from any Huh-7 cellular sample (data not shown) which is surprising considering the positive CD44 immunofluorescence results shown in Figure 4.12, but may reflect the relatively low level of CD44 expression in Huh-7 cells. However, strong knockdown of CD44 protein levels were seen for all 3 siRNA sequences at both
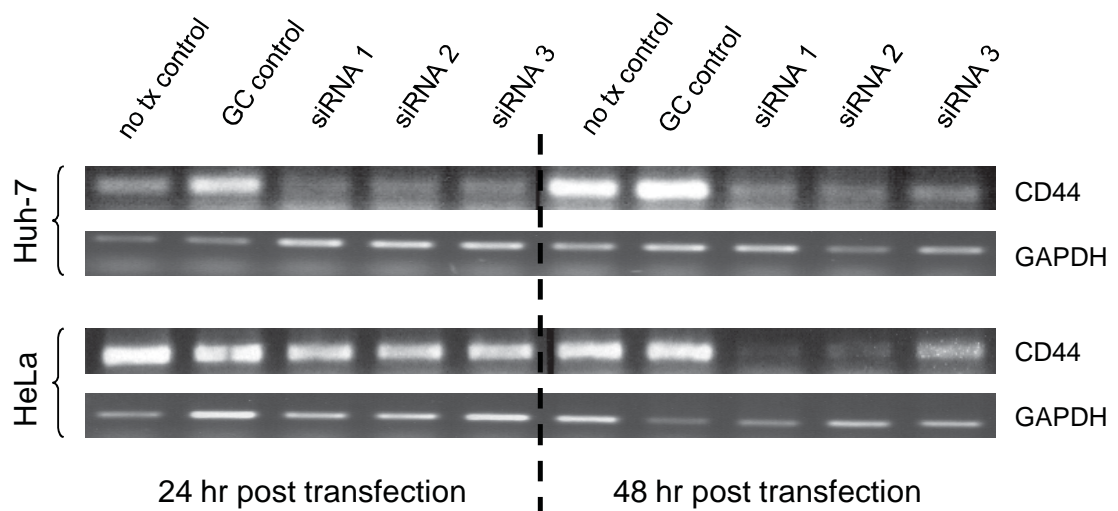
Figure 4.17 All three CD44 siRNA sequences produced distinct knock-down of CD44 mRNA at 24 and 48 hours post transfection in Huh-7 cells, and at 48 hours post transfection in HeLa cells. Slight knockdown for all thee siRNA sequences is seen in HeLa cells 24 hours post transfection.

24 and 48 hours post transfection in HeLa cells compared to both untransfected and scrambled siRNA transfected controls (Figure 4.18). Therefore, by knocking down mRNA expression of CD44 by siRNA transfection, protein expression is also abrogated. siRNA 1 and siRNA2 were chosen for further studies due to their ability to strongly suppress both mRNA and protein expression of CD44 in HeLa cell lines and mRNA in Huh-7 cells. Given the strong knock-down of CD44 protein in HeLa cells, it was assumed that knock-down of CD44 protein was also occurring in Huh-7 cells.

To confirm that siRNA-mediated knockdown of CD44 could be maintained over the full time period of the cellular proliferation assay, CD44 mRNA and protein levels were monitored at 24 hour timepoints over 4 days post transfection. Total cellular RNA was harvested at 1, 2, 3, and 4 days post transfection, cDNA prepared and CD44 expression levels monitored as described above. Both siRNA 1 and 2 showed strong knockdown up to day 3 post transfection in Huh-7 cells (Figure 4.19 top), after which CD44 mRNA expression returned at day 4. In HeLa cells, knockdown was seen for both siRNA 1 and 2 at days 2-4 post transfection (Figure 4.19 bottom). Total cellular protein was also harvested at similar timepoints and CD44 expression evaluated by Western Blotting using an anti-CD44 antibody (NeoMarkers). Again, clear bands could not be obtained from any Huh-7 cellular sample (data not shown), however CD44 protein levels were severely decreased for both siRNA 1 and 2 at days 1-4 post transfection (Figure 4.20). These results clearly establish the knock-down of CD44 in HeLa cells and by inference Huh-7 cells.

4.2.7.5 Effect of siRNA knockdown of CD44 on OPN-induced increases in cellular proliferation

Having established CD44 knockdown we next wished to determine whether CD44 knockdown could abrogate OPN-mediated increases in proliferation of Huh-7 and HeLa cells. Cells were seeded in conditioned media from both naïve Huh-7 and OPN stably transfected (A8) cells. Three

Figure 4.18 All three CD44 siRNA sequences showed distinct knock-down of CD44 protein expression in HeLa cells at 24 and 48 hours post-transfection.

Figure 4.19 Both chosen CD44 siRNA sequences produced distinct knock-down of CD44 mRNA for up to 3 days in Huh-7 (days 1-3) and HeLa (days 2-4) cells.
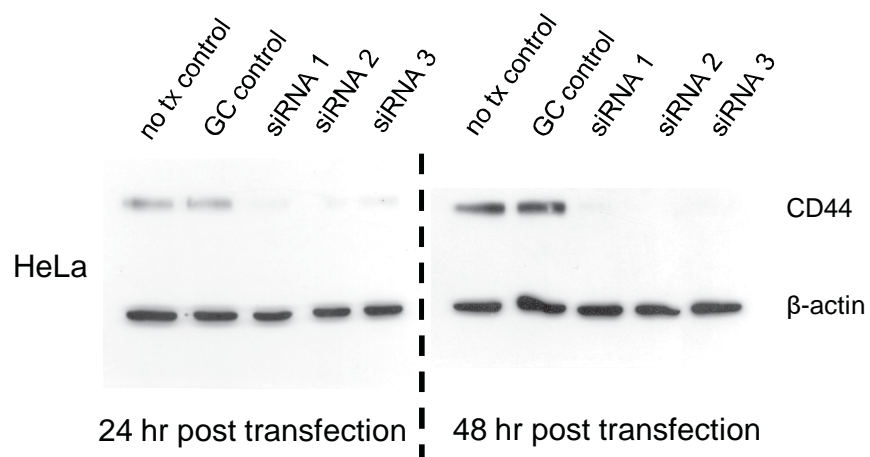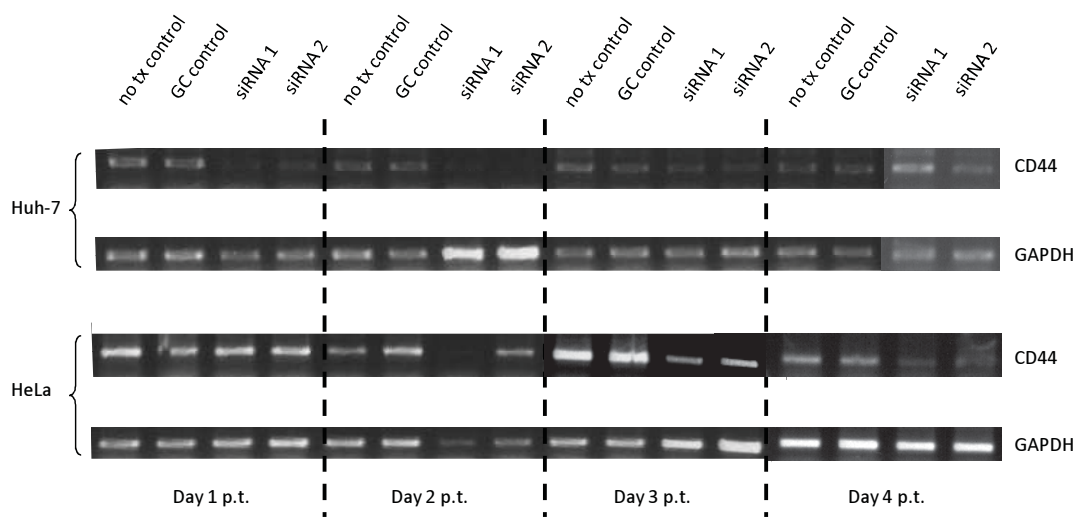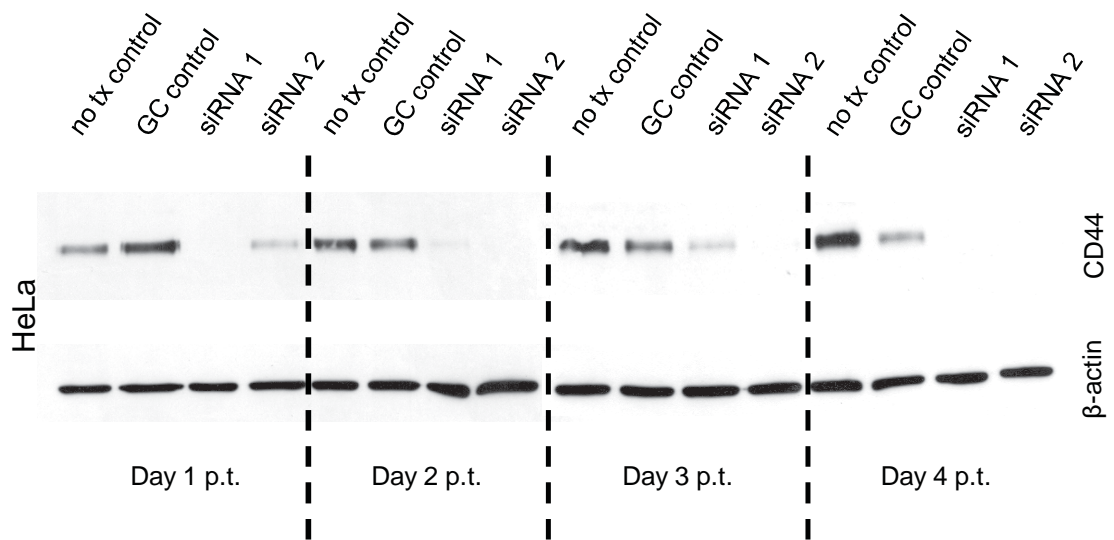
Figure 4.20 Both selected CD44 siRNA sequences showed distinct knock-down of CD44 protein expression in HeLa cells for 4 days post-transfection.

sets of wells were plated; one in cultured media alone, a second in cultured media plus CD44 siRNA 1 (CD44-HSS101596, Invitrogen), and a third in cultured media plus the scrambled Med GC control siRNA (Invitrogen). Cells were transfected with siRNA using the reverse transfection method provided by the manufacturer, whereby siRNA, Lipofectamine 2000^{TM} transfection reagent (Invitrogen) and serum-free media were incubated in the wells prior to the plating of cells. This reverse transfection method allows the proliferation assays to be performed exactly the same as all previous assays, without the need of allowing cells to adhere to the bottom of the well for 24 hours prior to transfection.

No difference in cellular proliferation was observed for Huh-7 cells grown in Huh-7 conditioned media in the presence of control siRNA or CD44 siRNA sequences compared to Huh-7 alone (Figure 4.21a black dashed lines). However, naïve Huh-7 cells grown in OPN-A conditioned media alone showed a significant increase in cell number on days 3 and 4 of growth (as previously demonstrated, see Figure 4.9) as did those in the presence of control siRNA (Figure 21a blue and purple respectively, $p < 0.05$). However, transfection with CD44 siRNA resulted in no observable increase in proliferation when cells were concurrently subjected to OPN-A conditioned media (Figure 4.21a orange). A similar result was observed for HeLa cells (Figure 21b). This experiment was repeated for both cell lines with transfection of siRNA 2 (CD44-HSS101597, Invitrogen) with similar results obtained (data not shown). This result, along with that of Section 4.2.7.2, strongly suggests a role for the CD44 in OPN-mediated proliferation of Huh-7 and HeLa cells.

4.2.7.6 Effect of blocking CD44-OPN interactions on OPN-mediated increases in carcinoma cell proliferation

To further confirm the above results, an anti-CD44 antibody known to block the active site of CD44 (Teramoto et al., 2005) was used to prevent binding of OPN to CD44. Naïve Huh-7 cells
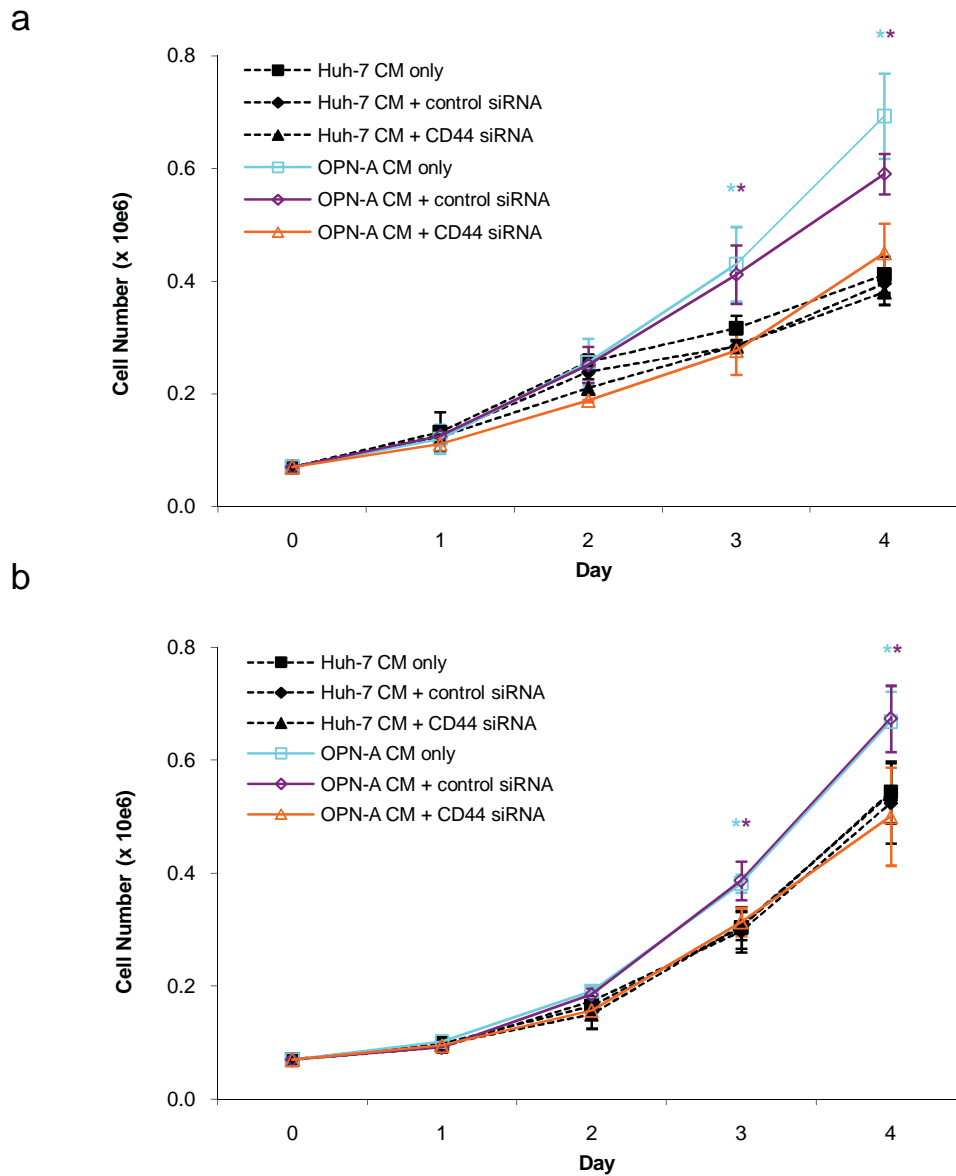
Figure 4.21 Knockdown of CD44 expression abrogates OPN-mediated increases in cellular proliferation in both Huh-7 **(a)** and HeLa **(b)** cell lines. Both Huh-7 and HeLa cells grown in OPN-A cultured media alone and with a control siRNA showed increased cellular growth over cells grown in the absence of OPN, however the addition of CD44 siRNA abrogated this effect in both cell lines. Huh-7 CM = cultured media from naïve Huh-7 cells. OPN-A CM = cultured media from OPN-A stable cells. * $p < 0.05$.

were seeded in conditioned media from both parental Huh-7 and OPN-A stably transfected (A8) cells. Three sets of cells were plated; one in conditioned media alone, a second in conditioned media with the addition of an anti-CD44 blocking antibody (H-CAM [300], Santa Cruz Biotechnology), and a third in conditioned media with the addition of a redundant antibody of the same isotype as anti-CD44 (unrelated rabbit IgG, Santa Cruz Biotechnology). This redundant antibody was used as a control to negate any effect seen from the addition of antibody to conditioned media.

No difference in cell number was observed for Huh-7 cells grown in Huh-7 conditioned media irrespective of the presence or absence of either antibody (Figure 4.22a black dashed lines), indicating that the binding of the CD44 H-CAM antibody does not activate the CD44 receptor leading to increased growth. Naïve Huh-7 cells grown in OPN-A conditioned media alone and in the presence of isotype control antibody both showed significantly increased cell number on days 3 and 4 of growth compared to Huh-7 cells grown in Huh-7 conditioned media (Figure 4.22a blue and purple lines respectively, $p < 0.05$), however the addition of an anti-CD44 H-CAM antibody resulted in no observable increase in proliferation (Figure 4.22a orange line). The above experiment was repeated using the high-CD44 expressing cell line HeLa with similar results (Figure 4.22b, $p < 0.05$). Both cell lines were tested with conditioned media from a second set of clones with similar results (data not shown, $p < 0.05$). These results strengthen the claim that the OPN-CD44 interaction plays a major role in proliferation of Huh-7 and HeLa cells.

4.2.8 Effect of OPN on CD44 expression

The results of this chapter strongly suggest that OPN-mediated increases in hepatoma cell proliferation occur through interactions with surface-expressed CD44. However, they do not suggest whether this process is limited by the number of CD44 receptors expressed on the hepatoma cell surface or if OPN expression and binding to CD44 activates a feedback loop

101
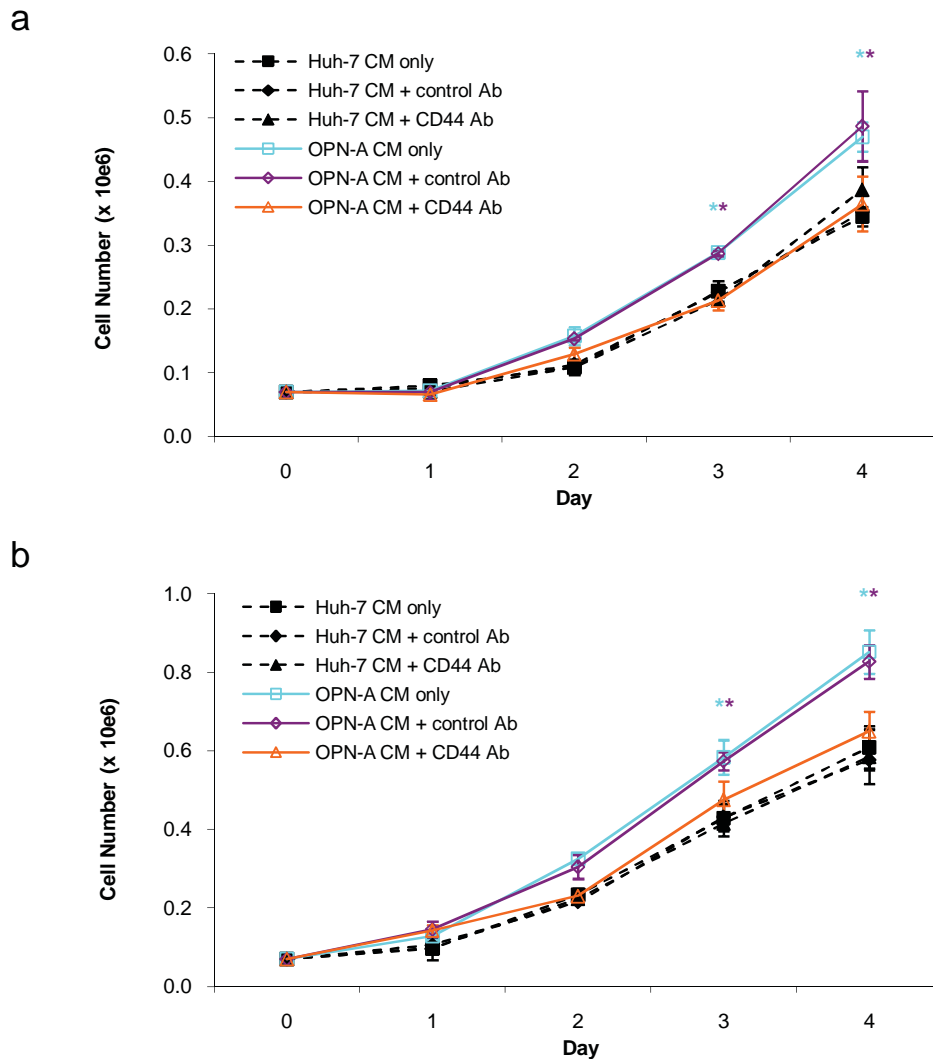
Figure 4.22 Addition of anti-CD44 antibody to conditioned media from OPN-A expressing cells blocks the paracrine effect of secreted OPN on cellular growth of Huh-7 **(a)** and HeLa **(b)** cells. Both Huh-7 and HeLa cell lines with OPN-A conditioned media alone and with an isotype control antibody showed increased growth over baseline controls, however addition of anti-CD44 antibody abrogated this increased growth. The addition of isotype control or anti-CD44 antibodies to Huh-7 conditioned media did not affect the growth of Huh-7 cells. CM = conditioned media. * $p < 0.05$.

whereby CD44 transcription and translation is upregulated to enhance the subsequent proliferative effect. A previous study suggested that the binding of OPN to CD44 v6/7 induces transcription of CD44 and subsequently increases cell surface expression of CD44s, v6 and v9 (Khan et al., 2005). To investigate the possibility of increased CD44 transcription from OPN binding in our system, Huh-7 cells were seeded in 6-well tissue culture plates and subjected to conditioned media from either naïve Huh-7 or OPN-A transfectant cells for increasing timepoints up to 48 hours. RNA was harvested and subjected to RT-PCR for CD44 mRNA expression. After normalising expression to that obtained for GAPDH, no change in CD44 expression was observed between Huh-7 cells cultured with or without OPN at any timepoint (Figure 4.23). Therefore, under our experimental conditions the binding of OPN does not affect transcription of CD44.

4.3   Discussion

4.3.1   OPN increases proliferation of hepatoma cell lines in a paracrine manner through interaction with CD44

The role of OPN in cellular proliferation is a controversial topic, with contrasting results reported for a range of cultured carcinoma cell lines. In particular, the roles of the alternatively spliced variants OPN-B and –C in relation to cellular proliferation remain completely uncharacterised apart from a single study showing no effect of OPN-C expression on proliferation of a breast cancer cell line (He et al., 2006). This chapter outlines the successful construction of expression vectors for each of the three OPN variants, with subsequent production of stable Huh-7 cell lines expressing each of the variants. Expression of OPN was confirmed by RT-PCR, ELISA and western blotting. This panel of cell lines allowed us to thoroughly investigate the role of each OPN variant in Huh-7 proliferation.

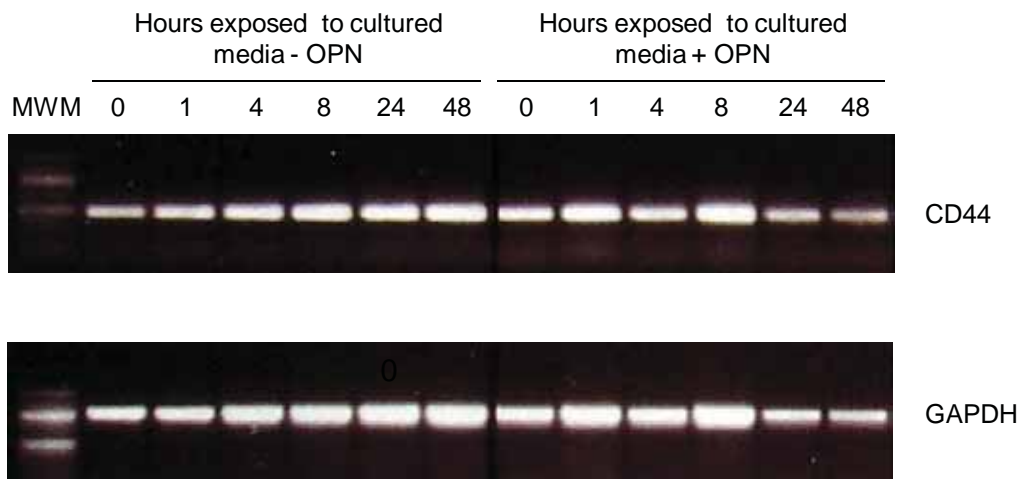**Figure 4.23** OPN expression does not affect CD44 expression in Huh-7 cells. Cells were grown in normal culture media, then exposed to cultured media from either naïve Huh-7 or OPN-A stable transfectant cells for up to 48 hours. After accounting for variances in GAPDH expression, no change in CD44 expression was observed between cells grown with or without OPN at any timepoint. MWM = 100 bp molecular weight marker.

The major finding of this chapter, and indeed this study, was the role of the OPN variants in *in vitro* proliferation and *in vivo* tumor growth of HCC (see Chapter 5). It is becoming increasingly clear that in addition to the role of OPN in the metastatic process it also has a role in cellular proliferation of a number of tumors. However, as mentioned previously its role in HCC is not well studied, and although a recent study using an siRNA OPN knock-down approach suggested that OPN is important for HCC proliferation (Sun, B. S. et al., 2008), neither the relative roles of OPN variants nor the cellular receptor responsible were investigated. In contrast to the above OPN knock-down study, we over-expressed the OPN variants in the HCC cell line Huh-7 and investigated cellular proliferation *in vitro*. Huh-7 cells were chosen for this study as they have a low basal level of OPN mRNA expression and undetectable OPN expression as detected by ELISA or immunoblotting (as confirmed during this study). It should be noted that while we refer to these cell lines as over-expressing OPN (and variants), this is not necessarily the case as in a physiological HCC setting OPN mRNA and protein expression are often expressed at levels well above that of baseline OPN expression. Stable ectopic expression of OPN-A, -B and –C resulted in secretion of all OPN forms into the culture media and significant proliferation of Huh-7 cells either directly or through the addition of conditioned media to naïve Huh-7 cells. This suggests that, at least *in vitro*, OPN exerts its proliferative effect in either an autocrine or paracrine manner that correlates with the secreted nature of this protein. Consistent with the proliferative nature of secreted OPN, other cell lines also responded to OPN conditioned media including HepG2 and HeLa but not Hep3B (the reasons for this are discussed below). This autocrine/paracrine effect of OPN was confirmed through the use of a neutralising OPN antibody that abolished the proliferative effect of conditioned media. Interestingly, all OPN variants increased Huh-7 cell growth at a similar rate which suggests that, at least *in vitro*, all OPN variants can exert cellular proliferation potential. This is not inconceivable as the deletion of exons 4 (OPN-C) and 5 (OPN-B) do not impact on the integrin RGD domain or the CD44 binding domain, both of which

have the potential to play a role in receptor ligand-increased cellular proliferation. These results also suggest that removal of exons 4 and 5 does not impact on the tertiary structure of the protein at least within the integrin and CD44 binding domains. To our knowledge this is the first report that OPN and its variants play a significant role in cellular proliferation and growth of HCC *in vitro* in addition to OPN's reported role in the metastatic process.

To further elucidate the cellular pathways through which this OPN dependent proliferation occurs, we investigated the role of CD44 in this process. CD44 is one of two known OPN receptors (the other being integrins), and OPN-CD44 binding has previously been shown to induce chemotaxis, down-regulate IL-10 expression and confer metastatic behaviour on carcinoma cells (Gunthert et al., 1991; Rudy et al., 1993; Weber et al., 1996; Katagiri et al., 1999; Ashkar et al., 2000; Denhardt, Giachelli et al., 2001; Weber 2001). The C-terminal region of OPN can specifically interact with CD44v6 and or v7 to mediate cellular chemotaxis (Weber et al., 1996) and a thrombin-cleaved C-terminal OPN fragment induces macrophage migration via CD44 (Weber et al., 2002). While OPN CD44v6-7 binding has been associated with metastasis and invasion, little work has been done in regard to the CD44-OPN interaction and tumor growth, although one study revealed that knockdown of CD44 expression reduces tumor growth in colon carcinoma cells (Harada et al., 2001). In this chapter we showed that the increased growth rate of Huh-7 cells in response to OPN conditioned media was as a result of CD44 expression, as blocking CD44 with a neutralising antibody completely abolished this growth effect. Furthermore, HepG2 and HeLa cells which both express CD44v6/7 also showed this proliferative growth effect while the Hep3B cell line, which is negative for CD44v6/7, was unresponsive to OPN conditioned media. To conclusively demonstrate a role for CD44, an siRNA approach was employed that successfully reduced CD44 expression in both Huh-7 and HeLa cells. Consistent with the above results this reduction in CD44 in both cell lines resulted in a decrease in cellular

proliferation in response to OPN conditioned media. To our knowledge this is the first report that shows that the interaction between OPN and CD44 results in signals that drive cellular proliferation. This is not surprising considering that OPN interaction with CD44 has been shown to drive activation of the PI 3-kinase AKT pathway that may mediate survival and growth signals for HCC proliferation (Chakraborty et al., 2006). Moreover, it was recently shown that silencing of OPN in HCC derived cell lines could inhibit activation of the MAPK and ERK1/2 pathways, suggesting that OPN may regulate cell growth through activation of the MAPK signal transduction pathway (Sun, B. S. et al., 2008). However, the upstream factors responsible for this activation were not identified and further studies are required to determine the role of the OPN-CD44 interaction in the activation of growth signals in HCC.

In conclusion, the results of this chapter suggest for the first time that (i) OPN and its variants have the ability to accelerate proliferation of cultured HCC cell lines in a paracrine manner when expressed at high levels, and (ii) that this proliferative effect occurs through interaction with the cellular receptor CD44 (as demonstrated with OPN-A). This novel finding proposes a mechanism through which increased OPN may accelerate the growth of carcinoma cells *in vitro*, which in turn may suggest a mechanism for increased tumor growth in patients with high OPN levels. The *in vivo* effect of OPN on HCC tumor growth will be analysed in Chapter 5 of this thesis.

4.3.2   Future directions

This chapter clearly indicates a role for OPN in cellular proliferation, however as with most investigations this work also opens the door to many more questions. One such question that has not been addressed is the role of intracellular OPN. While OPN is readily secreted, intracellular OPN expression is noted in HCC (by IHC) and in many other tumors. Preliminary attempts to visualise intracellular OPN in Huh-7 stable cell lines in this thesis suggested that the different OPN variants may have different cellular locales. Visualisation of OPN variants within the cell is

inherently difficult due to the highly secreted nature of the protein, however future studies could use blockers of secretion (i.e., Brefeldin-A) to prevent OPN secretion allowing for easier sub-cellular visualisation and further evaluation of the cellular role of OPN.

Our results clearly suggest, for the first time, that the interaction between OPN and CD44 is a requirement for OPN-mediated increases in the cellular proliferation of HCC cell lines, however the molecular mechanisms responsible for this proliferative effect following receptor ligand interaction were not examined. OPN binding to either the integrins and/or CD44 initiates a complex activation of cellular signaling pathways involving NF-κB, Akt and MAPK activation, leading to growth, metastasis and angiogenesis effects (Chakraborty et al., 2006). Future studies should focus on which pathways are activated following OPN binding to CD44 through the use of genome wide profiling, dominant negative signaling proteins, knock-out cell lines and the use of specific chemical inhibitors. Interactions between $\alpha_v\beta_3$ integrin and OPN have previously been shown to be important in tumor growth (Wai and Kuo 2004), so it would therefore be of interest to investigate whether integrins (the other OPN receptor) play a similar role in OPN-mediated cellular proliferation by repeating all CD44 experiments with integrin-expressing cell lines and anti-integrin siRNA sequences and neutralising antibodies. Elucidation of the molecular events that lead to increased cellular growth could prove to be important in the search for novel targeted therapies in the treatment not only of HCC but other cancers.

CHAPTER 5: Effect of osteopontin expression on subcutaneous tumor growth *in vivo* in a nude Balb/C mouse model

5.1 Introduction

OPN has been widely reported as playing a number of important roles during carcinogenesis, including angiogenesis, metastasis and tumor cell proliferation. OPN's role in tumor metastasis has been well described, with both *in vitro* cell culture and *in vivo* tumor xenograft models outlining the effect of OPN on metastatic potential and malignant invasion as described elsewhere in this thesis (Section 1.3.6). Studies have also shown strong correlation between patient OPN levels and metastatic disease. High levels of OPN have been seen in patients with a range of cancer types, and links between increasing OPN expression and increasing tumor burden (Kon et al., 2000; Fedarko et al., 2001) and poorer clinical outcome (Tuck et al., 1998) suggest that OPN is somehow involved in tumor progression. However, the role of OPN in accelerating tumor cell growth remains unclear.

The results of Chapter 4 of this thesis strongly suggest that OPN and its variants play a role in accelerating proliferation of HCC derived cell lines *in vitro*. However, understanding this phenomenon in an *in vivo* growth model will confirm our *in vitro* data in a more physiological setting and provide a future platform to study OPN biology *in vivo*. It has been suggested that tumor cell-derived OPN (as opposed to that expressed from resident macrophages) enhances tumor growth (Crawford, H. C. et al., 1998), and previous xenograft models of human colon (Irby et al., 2004) and lung (Cui et al., 2007) cancer have indicated that OPN over-expression increases tumor growth in a murine model. However, the growth regulating properties of OPN in relation to HCC have not been well studied in *in vivo* models.

Previous results of this thesis (Chapter 4) suggest that OPN has a positive effect on the growth rate of tumor derived cells *in vitro*. This chapter **aims to develop and characterise a model of Huh-7 derived xenograft growth in nude Balb/c mice that will allow us to evaluate whether OPN and its variants can increase the growth rate of Huh-7 cells** *in vivo***.**

5.2   Results

5.2.1   Development of subcutaneous Huh-7 xenograft tumors in nude Balb/c mice

Murine tumor growth models are widely used in human cancer research as an investigative tool to examine factors affecting malignant growth, transformation, invasion and metastasis, and the tumor response to novel anti-cancer agents. These tumor growth models involve the implantation of either solid tumor pieces or cultured tumor-derived cells into immuno-deficient mice under the skin (subcutaneous) or within/adjacent to internal organs (orthotopic). Human tumor growth in a murine model is made possible by the fact that, due to a mutation in the *Foxn1* gene, athymic mice do not possess a thymus and therefore do not produce mature T cells (Flanagan 1966; Nehls et al., 1994). The lack of mature T cells results in an inability to distinguish between "self" and "non-self" tissues and therefore tolerance of human cell and tissues by the murine immune system.

The basic murine xenograft model can be adapted for use with almost any carcinogenic human cell line. Numerous groups have developed their own in-house methods for initiating tumor growth from subcutaneous injection of Huh-7 cells. Previous studies indicate that subcutaneous injection of $1 - 5 \times 10^6$ Huh-7 cells into 4 - 8 week old nude Balb/c mice (of either sex) can result in visible tumors 5 - 22 days post injection (Table 5.1).

Huh-7 cells injected	Animal age (weeks)	Sex	Day of tumor appearance	Reference
2×10^6	4-6	F	5	(Qin et al., 1998)
1×10^6	5	M	10-14	(Kito et al., 2003)
4×10^6	6-8	F	22	(Kern et al., 2004)
1×10^6	4	M	12	(Yu, J. et al., 2006)
5×10^6	6	F	5-10	(Lin, L. et al., 2009)

Table 5.1 Review of previous studies which have optimised xenograft growth from subcutaneous Huh-7 injection in athymic mice

As Huh-7 cells vary between laboratories, it was imperative to assess their ability to form tumors in our hands. Varying concentrations of Huh-7 cells were injected into 5 week old female nude Balb/c mice in order to develop an in-house model for Huh-7 initiated murine xenograft growth. Cells were cultured under normal conditions, harvested with trypsin, counted using trypan blue exclusion and resuspended in sterile PBS. Duplicate 100 μL cell aliquots containing 5×10^5, 1×10^6, 2×10^6, 5×10^6, and 1×10^7 cells were prepared and injected subcutaneously into both dorsal flanks of one mouse per group. Cells were carefully injected between the skin and peritoneal cavity using a sterile 1 mL syringe and 26 G needle (Figure 5.1). Mice were observed daily for the visible presence of tumors at the injection site and tumor width and length measurements taken daily thereafter to monitor tumor growth.

In the mouse injected with 5×10^5 cells, no tumors were visible by termination of the experiment (84 days post injection). Injection of all other Huh-7 cell numbers gave rise to at least one visible tumor by day 39 post injection (Table 5.2). 5×10^6 was the only cell number that gave rise to tumors at both injection sites.
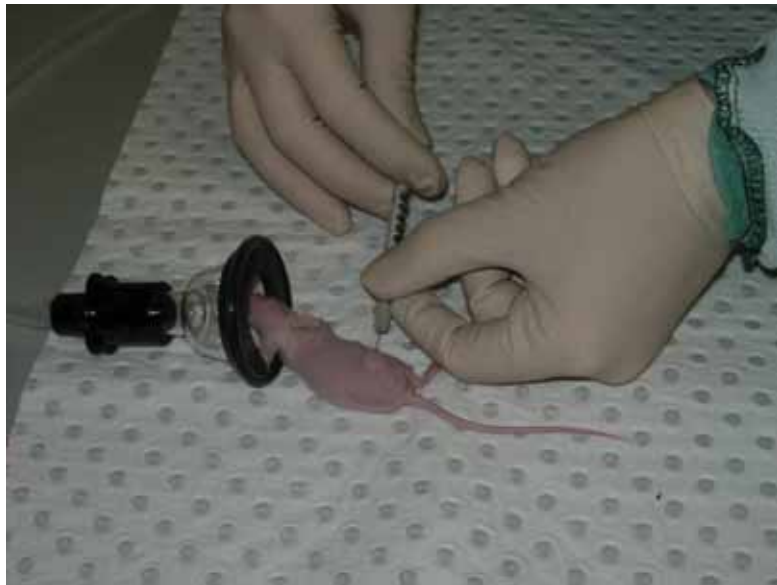
Figure 5.1 Subcutaneous injection of Huh-7 cells into the hind flank of a female Balb/c nude mouse aged 5 weeks. Mice were placed under anaesthesia during all injections. Cells were injected between the skin and peritoneal cavity using a sterile syringe and needle.

Huh-7 cells injected	Day of tumor appearance
5×10^5	-
1×10^6	39
2×10^6	32
5×10^6	24 and 35
1×10^7	18

Table 5.2 Day of first appearance of subcutaneous tumors initiated from Huh-7 cell injection into nude Balb/c mice

Once sighted, tumors grew steadily and were excised from euthanised animals once they had grown to 10 mm in one dimension. Representative pictures (from a mouse injected with 5×10^6 Huh-7 cells) indicate that the tumors grew in a uniform manner and were deep red in colour (Figure 5.2a and b). Haematoxylin and eosin (H&E) staining of the tumor revealed it consisted of highly dilated blood-filled vessels surrounded by solid tumor that contained actively dividing cells (as determined by the visualisation of numerous mitotic spindles; Figure 5.2c and d). By virtue of being the only cell number to show steadily growing tumors from both samples injected, 5×10^6 cells was deemed optimal for initiation of Huh-7 derived xenografts in nude Balb/c mice. This cell number correlates with that used in other studies as mentioned previously in this chapter.

The albumin status of harvested Huh-7 derived tumors was assessed using human specific albumin primers to confirm the human origin of the tumors. A portion of harvested tumor initiated from 5×10^6 Huh-7 cells was homogenised and total RNA extracted using Trizol®. cDNA was prepared and subjected to PCR using primers specific for human albumin (see Table 2.1). The Huh-7 derived tumor was positive for human albumin, indicating the tumor contained
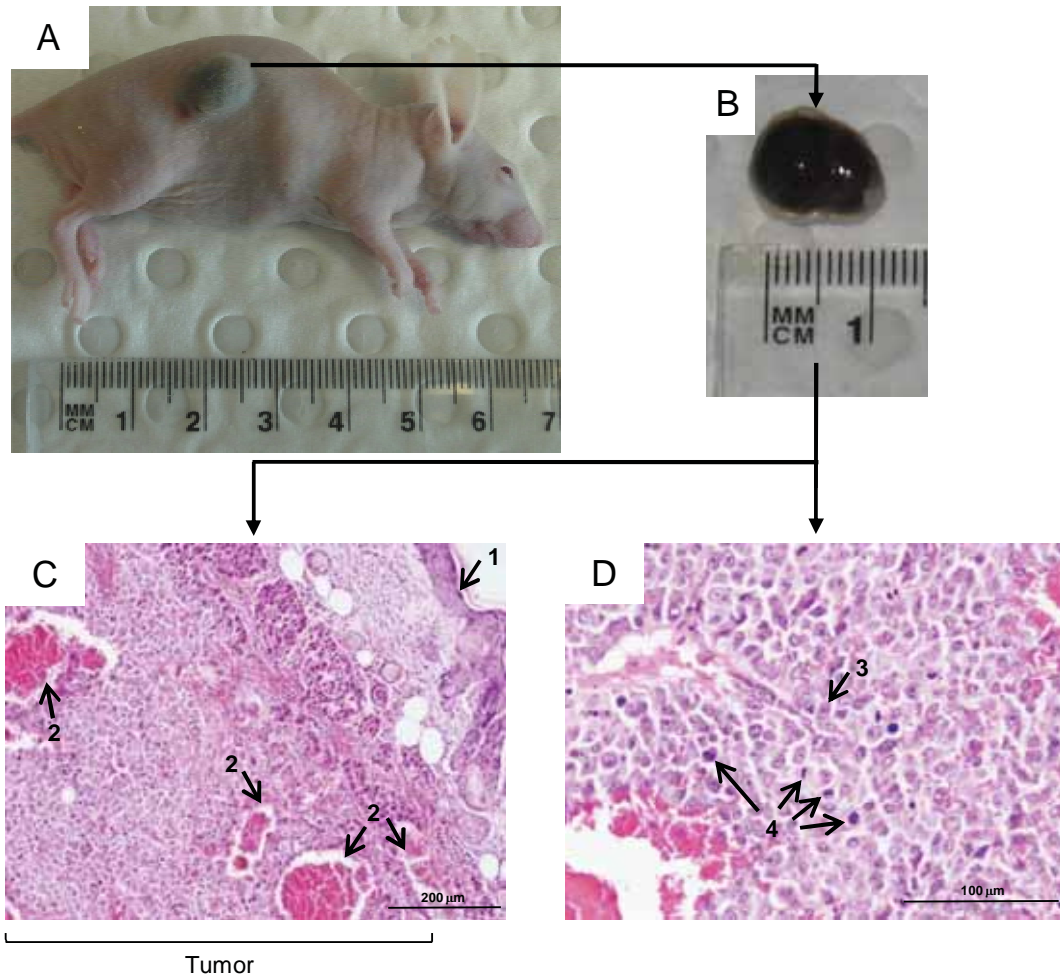
Figure 5.2 (a) Representative Huh-7 tumor xenograft in a nude Balb/c mouse. This tumor

was initiated from subcutaneous injection of 5×10^6 Huh-7 cells. **(b)** Note the uniform

deep red colour, suggesting high levels of tumor vascularisation. A H&E stain was

performed on sections taken from this tumor. **(c)** Low magnification of the Huh-7 derived

tumor and its location within the murine tissue. Note the proximity of the tumor to the

mouse skin (**1**→) The highly vascular nature of the tumor is confirmed by the presence of

numerous highly dilated venules (**2**→). **(d)** Higher magnification of the Huh-7 derived

tumor. Tumorigenic hepatocytes are easily identifiable (**3**→). The presence of numerous

mitotic spindles suggests that tumor cell division is active as expected (**4**→).

cells of human origin (Figure 5.3). No product was detected in normal mouse liver, confirming that the primers were specific for human, but not mouse, albumin.

5.2.2   Effect of OPN on Huh-7 derived xenograft growth

The aim of this chapter was to determine if OPN can exert its growth promotion effect in the setting of a proliferating tumor *in vivo*. The role of OPN in tumor cell growth is controversial and moreover there is a lack of information regarding OPN expression and HCC growth and no information investigating the relative roles of the OPN variants in this process. This study will investigate whether an increase in Huh-7 *in vivo* tumor growth is modulated by increased OPN expression, including the alternatively spliced variants OPN-B and OPN-C.

The effect of OPN on xenograft growth was investigated by comparing the growth of tumors initiated from Huh-7 cells expressing the three OPN variants with that of mock transfected (i.e. transfected with empty pRc/CMV) Huh-7 derived tumors. Mock transfected Huh-7 cells (Huh-7/mock) were used for comparison rather than naïve Huh-7 cells to ensure that all cell lines were subjected to identical selection and growth conditions prior to injection. Stable Huh-7/mock, OPN-A, OPN-B and OPN-C transfectant Huh-7 cell lines (representing clones used previously in this study for cellular proliferation experiments) were cultured under normal conditions, trypsinised, counted using trypan blue exclusion and resuspended in sterile PBS. Duplicate 100 μL cell aliquots containing 5×10^6 cells were prepared and injected subcutaneously into both dorsal flanks of groups of five (Huh-7/mock) or eight (OPN transfectants) mice. Animals were monitored daily for the visual appearance of tumors on either flank, and tumor width and length measurements recorded with calipers daily thereafter, allowing for tumor volumes to be calculated. Tumor take rate ranged from 70 - 87.5% (Table 5.3).
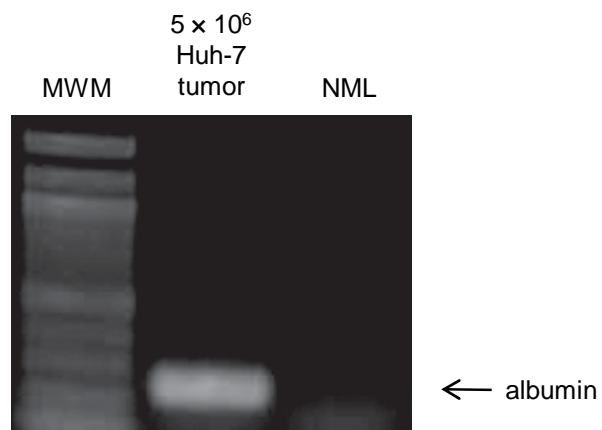
Figure 5.3 Human albumin PCR on a Huh-7 derived xenograft from a nude mouse injected with 5 x 10^6 Huh-7 cells. The presence of human albumin confirms that the tumor contains cells of human origin. These primers only bind human albumin and not murine albumin as shown by the lack of expression seen in normal mouse liver (NML). MWM = 100 bp molecular weight marker.

Cell line	Tumors	Injection sites	Take rate (%)
Huh-7/mock	7	10	70
OPN-A	14	16	87.5
OPN-B	13	16	81.25
OPN-C	14	16	87.5

Table 5.3 Tumor take rate of transfectant Huh-7 derived cell lines in a nude mouse xenograft growth model

Day of tumor appearance was noted as the day the tumor was first visible to the naked eye and measurable with calipers. On average, OPN-A derived tumors appeared at 7 days post injection, followed by OPN-B, OPN-C and Huh-7/mock at days 12 - 16 (Figure 5.4). OPN-A derived tumors were the only OPN expressing tumors to appear significantly earlier than control Huh-7/mock ($p < 0.0001$), although a trend was also evident for the earlier appearance of OPN-B and OPN-C tumors.

Tumor volume was monitored daily and graphed to indicate the tumor growth rate of each transfectant cell line group until the day of culling (Figure 5.5). All three OPN expressing tumor groups grew faster and larger than the control Huh-7/mock group, however this accelerated growth was significantly higher for OPN-A only ($p < 0.02$ for days 8-18 of tumor growth). It is interesting to note that once established, tumors for OPN-B and –C expressing Huh-7 cells rapidly increased their tumor volume similar to that of OPN-A derived tumours. This suggests that once established, tumors expressing any of the OPN variants may proliferate at similar rates. Experiments were repeated with a second set of OPN expressing clones with similar results observed (data not shown). This ensured that the observations above were not due to clonal selection bias.
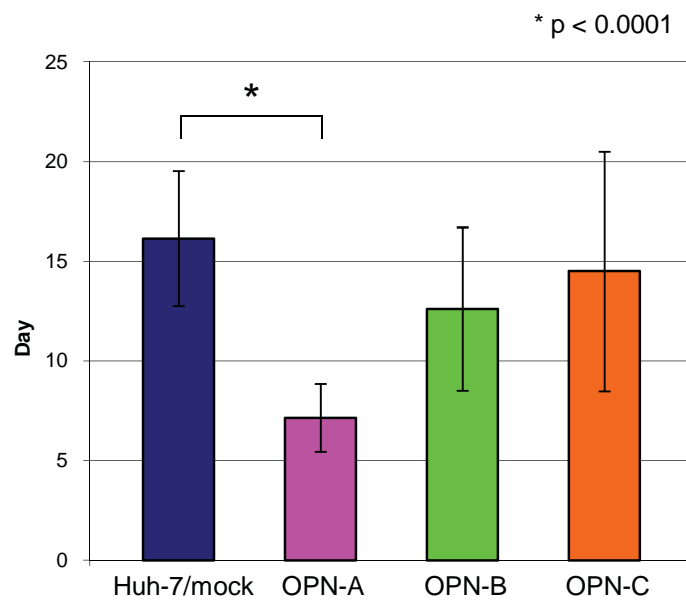
Figure 5.4 Average day of appearance of Huh-7 derived tumors with and without OPN variant overexpression. OPN-A tumors appeared first, followed by OPN-B, OPN-C and Huh-7/mock. OPN-A tumors appeared significantly earlier than Huh-7/mock tumors.
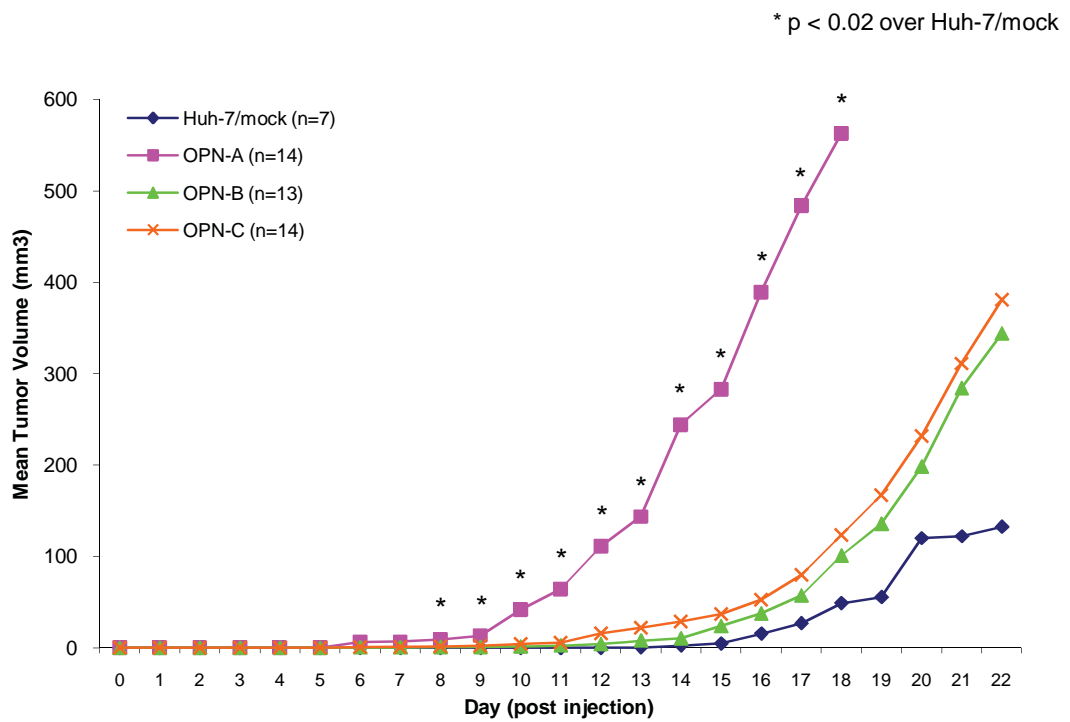
Figure 5.5 Average growth of nude mouse xenografts initiated from Huh-7 transfectant cell lines over-expressing the three OPN splice variants compared to a control mock transfectant Huh-7 line. Tumors from all OPN transfectant lines grew faster and larger than control Huh-7/mock tumors once established. OPN-A tumor growth was significantly larger than control tumors for days 8-18 of growth.

Each group of animals was culled when at least one tumor in that group had dimensions above the acceptable size threshold set for this experiment (15 mm in one dimension); namely, day 18 post-injection for OPN-A and day 22 for all other groups. Visual tumor sizes on the day of termination for each group varied greatly, however tumor volume is clearly greater for OPN-A expressing Huh-7 cells compared to the other OPN expressing cells and Huh-7/mock control (Figure 5.6). Compared to Huh-7/mock tumors, tumors from OPN-A mice were much more deep red in colour, soft to palpate and appeared to be very vascular (Figure 5.6 top left). This is consistent with the increased growth rate of these tumors and may also reflect the fact that OPN has been suggested to have angiogenic properties during tumor growth (Hirama et al., 2003).

Portions of each tumor were harvested, stored in 10% buffered formalin and processed for histological analysis. 4 µm sections were cut and mounted onto glass sides for histological analysis. Representative tumor tissue from all OPN expressing tumors showed a higher density of tumor vasculature than the control Huh-7/mock tumors (Figure 5.7a, c, e and g), which correlates with the macroscopic appearance of the tumors described previously (Figure 5.6). High powered magnification of tumor sections indicated that a high proportion of OPN-expressing Huh-7 cells were in various stages of cell division, compared to control Huh-7/mock tumors as indicated by the increased presence of mitotic spindles (Figure 5.7b, d, f, and h). This observation correlates with our *in vitro* data from Chapter 4 suggesting that Huh-7 cell proliferation increases when expressing or exposed to any of the OPN variants. Interestingly OPN-A tumors had larger blood filled vessels and a greater area of necrotic tumor tissue as visualised by the presence of Huh-7 cells with highly condensed nuclei. This suggests that the high growth rate of OPN-A tumors could not keep up with an adequate blood supply, resulting in areas of hypoxia and tumor cell death (due to a lack of oxygen), and therefore increased areas of necrosis in these tumors compared to control Huh-7/mock and OPN-B and –C tumors. Chronic hypoxia due to accelerated
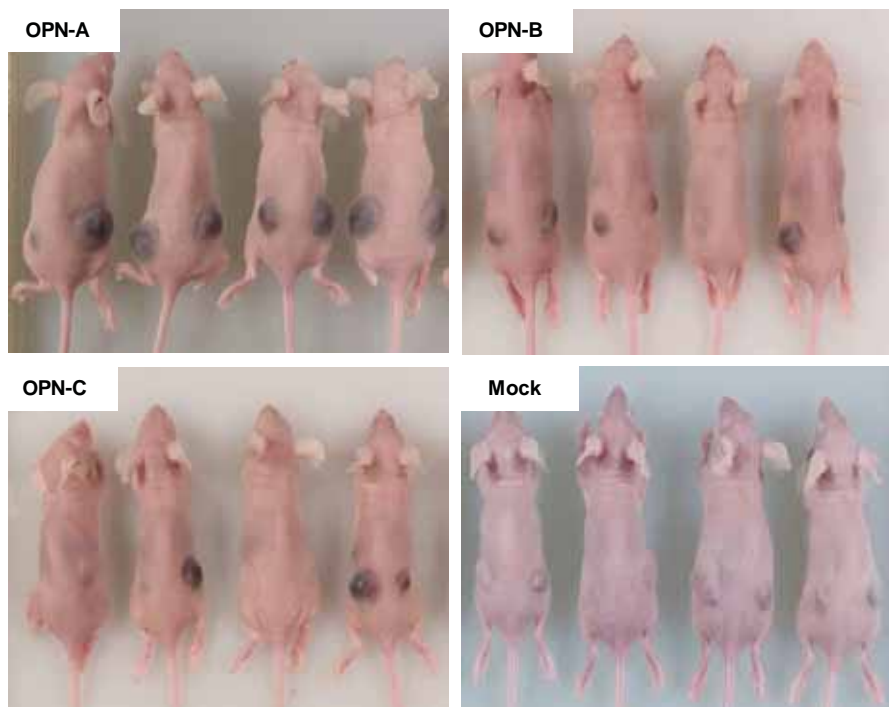
Figure 5.6 Representative visualisation of tumors on day of killing for each tumor group (day 18 for OPN-A, day 22 for all other groups). Tumors appear much larger for OPN-A than all other groups. Tumors for OPN-B and OPN-C also appear visually larger than the control group (Huh-7/mock). Tumors from all OPN groups appeared deep red colour, whilst those from the control group did not.

Figure 5.7 Representative H&E staining of Huh-7 derived tumor xenografts on day of killing for each group (day 18 for OPN-A, day 22 for all other groups) at $4 \times$ (top) and $20 \times$ (bottom) magnification. A higher density of tumor vasculature ($\mathbf{1}\rightarrow$) was observed for all OPN expressing tumors **(c, e, and g)** compared to control Huh-7/mock tumors **(a)**, which showed large areas lacking vasculature. Only one cell undergoing mitosis ($\mathbf{2}\rightarrow$) was observed in the Huh-7/mock tumor **(b)**, whereas numerous mitotic spindles were observed in tumor tissue of all OPN expressing tumors **(d, f, and h)**. The increased presence of mitotic spindles suggests that a higher proportion of tumorigenic hepatocytes are dividing in tumors expressing OPN than control tumors, which correlates with our *in vitro* data indicating that OPN expressing Huh-7 cells proliferate at a greater rate than naïve Huh-7 cells.

4 × magnification　　　　　**20 × magnification**
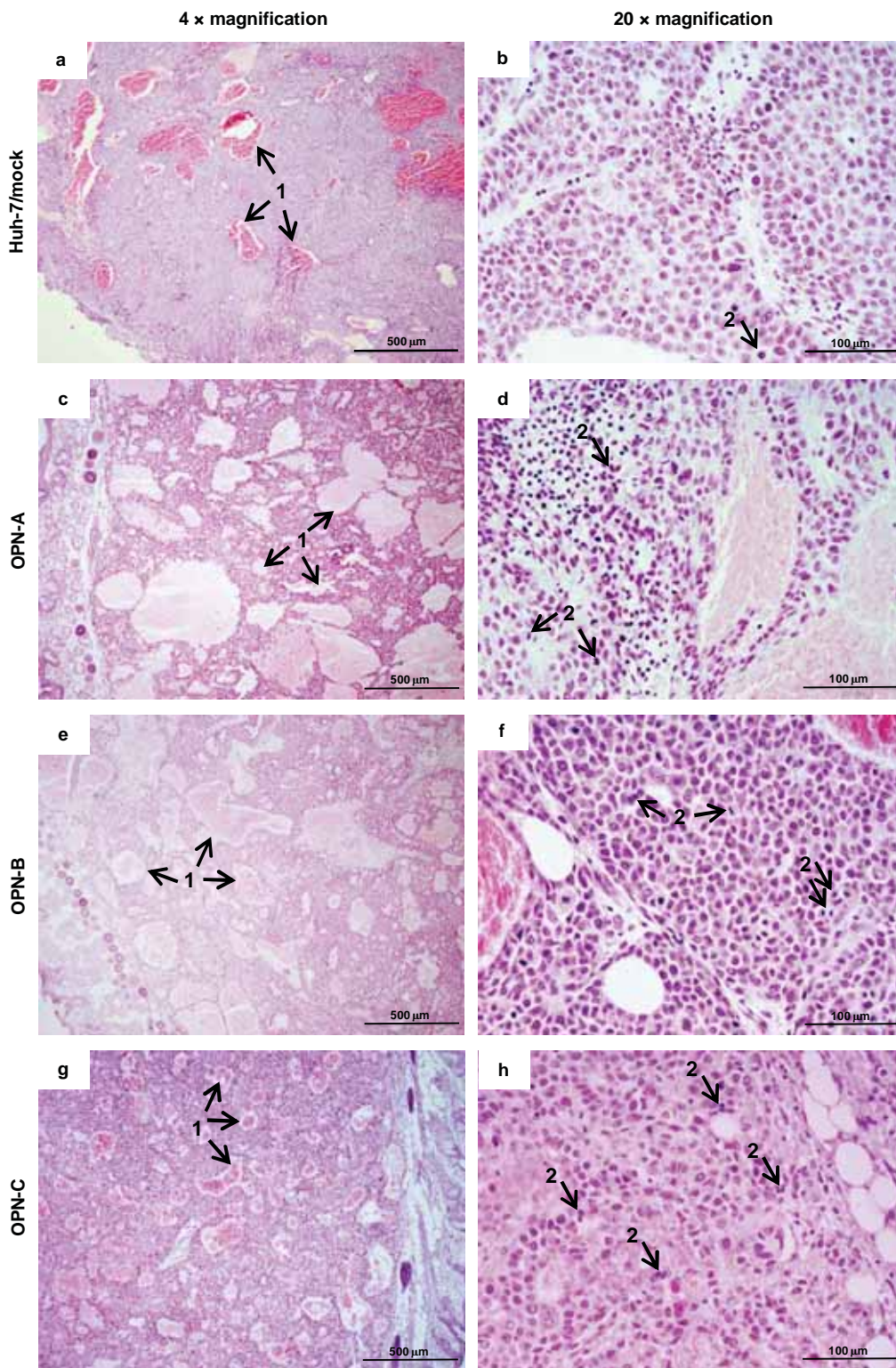
growth of tumor cells compared to endothelial cells required for blood vessel formation has been shown previously (Vaupel et al., 1989).

5.2.3 Detection of OPN expression and secretion in tumor xenografts derived from OPN stable transfectant cell lines

Detection of OPN expression within xenografts and circulating in blood was performed to ensure that the OPN transfectant cells growing and dividing within a tumor *in vivo* still expressed their corresponding OPN variant. This confirmation was performed in two parts: detection of OPN mRNA (by RT-PCR) and protein expression (by IHC) within the tumor tissue, and detection (by ELISA) of secreted human OPN in murine serum.

cDNA previously prepared for each tumor was subjected to RT-PCR for OPN using primers able to concurrently amplify all three transcript variants (see Table 2.1). Representative tumors from each OPN group showed strong expression of a single variant, matched to the specific OPN variant that the injected cells expressed (Figure 5.8). Tumors derived from Huh-7/mock cells showed low level expression of all three variants in a similar pattern to that seen previously in this thesis for cultured Huh-7 cells. Tumors initiated from OPN-B and OPN-C transfectants did however show low-level expression of OPN-A, which most likely reflects basal OPN-A expression in Huh-7 cells. Alternatively, it is possible that these OPN-A transcripts represent native murine OPN expression derived from murine cells within the tumor. Clearly OPN is being expressed at the mRNA level.

Detection of cellular retained OPN *in vitro* is difficult due to the secreted nature of OPN (Rittling and Novick 1997), however the cytoplasmic detection of OPN in cultured cells (see Figure 4.4) and HCC tissue (see Figure 3.1) prompted us to investigate OPN expression in xenograft tumor tissue by IHC. Tumor sections were immuno-stained for OPN using a rabbit α-OPN antibody or

114

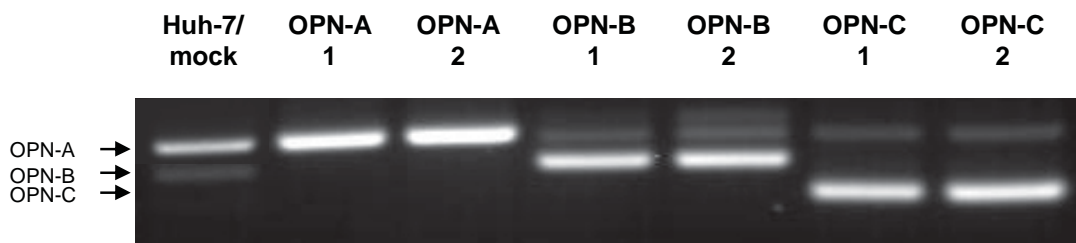**Figure 5.8** Representative tumors from all OPN over-expressing cell lines showed strong expression of their corresponding transcript variant. Huh-7/mock tumors showed a pattern of OPN variant expression similar to cultured Huh-7 cells as shown previously in this study. OPN-B and OPN-C tumors also showed weak expression of OPN-A which is thought to represent either basal Huh-7 OPN expression or native murine OPN.

normal rabbit IgG isotype as a control antibody (see Section 2.3.26 and Table 2.3). Sections from both Huh-7/mock and OPN-A tumors showed low background staining for the isotype control antibody (Figure 5.9). The Huh-7/mock tumor showed weak staining for OPN within the cytoplasm of tumorigenic hepatocytes which is above that of the isotype control. This is consistent with the low levels of mRNA expression seen in cultured Huh-7 cells and suggests that Huh-7 cells express a low basal level of OPN *in vivo*. However, the OPN-A expressing tumor showed significant OPN expression in the cytoplasm of tumorigenic hepatocytes and in the extracellular matrix. These results confirm that OPN-expressing Huh-7 cells do express OPN within the *in vivo* tumor.

OPN is naturally secreted and as our injected cell line OPN-A secretes large amounts of OPN, an in-house OPN sandwich ELISA was performed on serum harvested from tumor-bearing animals. Prior to injection with cultured cells for tumor growth, eye bleeds were performed on a number of animals and pooled. Serum was harvested by centrifugation at 2,000 rpm for 15 minutes at 4 °C and stored at -20 °C until required to provide a baseline sample for OPN ELISA testing. On the day of culling of tumor-bearing animals, blood harvest via heart venupuncture was performed under anaesthesia on all mice prior to euthanasia and tumor harvest. Serum was separated from each sample as previously described and stored at -20 °C. A human sandwich OPN ELISA (as previously described in Section 4.2.3) was performed to compare circulating serum OPN levels in animals bearing OPN over-expressing tumors to that of control (Huh-7/mock) animals, however secreted OPN could not be detected in any sample (data not shown). This human OPN ELISA was also performed on urine harvested from tumor-bearing animals at time of euthanasia, however OPN could not be detected in any sample (data not shown). The reasons for this are not apparent and require further investigation.

	Huh-7/ mock	OPN-A
α-OPN 1 μg/ml		
isotype control 1 μg/ml		
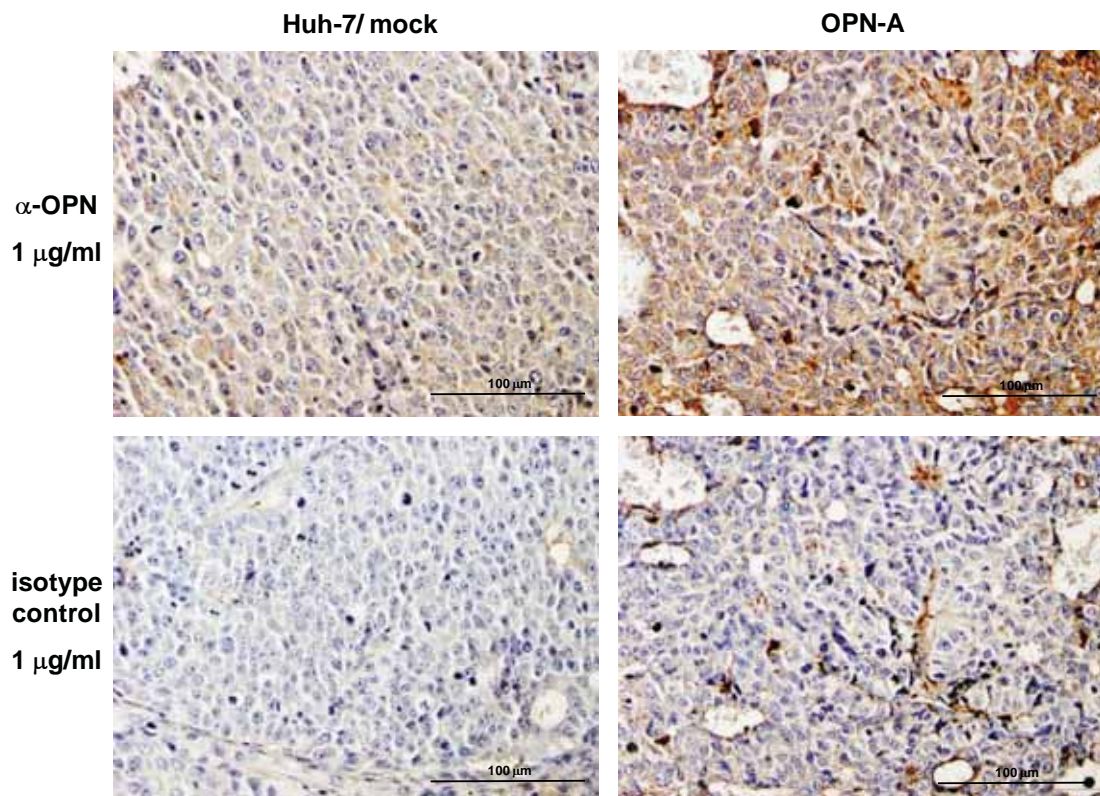
Figure 5.9 IHC staining of *in vivo* tumor sections derived from Huh-7 xenografts. OPN is significantly expressed in the cytoplasm of tumorigenic hepatocytes and within the extracellular matrix in mice injected with OPN-A expressing cells. A very low basal level of OPN is seen in the tumor derived from Huh-7/mock cells consistent with low level OPN mRNA expression noted in cultured Huh-7 cells. The isotype control antibody reveals a low level of background staining.

5.2.4 Effect of tumor OPN secretion on growth of neighbouring Huh-7 derived xenografts

Chapter 4 of this thesis determined that OPN secreted into conditioned media was able to increase the growth rate of cultured Huh-7 cells *in vitro* in an obvious paracrine manner (Section 4.2.6.2). This prompted us to determine whether OPN secreted from OPN expressing Huh-7 derived tumors could affect the growth of tumors derived from naïve Huh-7 cells.

To test this hypothesis, a pilot experiment was performed in which 5 nude Balb/c mice were injected (as previously described) with 5×10^6 naïve Huh-7 cells in their left dorsal flank and 5×10^6 OPN-A stable transfectant cells in their right dorsal flank (Huh-7 test; Fig 5.10). Growth rates of the naïve Huh-7 cells were compared to mice injected with Huh-7 cells injected into both flanks (Huh-7 control; Figure 5.10). This model should ascertain if OPN secreted from an OPN over-expressing tumor could affect growth of a naïve Huh-7 derived tumor at a distal site, and would also confirm the secretion of OPN from the tumor. As per the previous experiment, animals were monitored daily for the visual appearance of tumors with tumor width and length measured with calipers daily thereafter. Tumor take rate was at least 70% for all tumor groups (Table 5.4).

Cell line	Tumors	Injection sites	Take rate (%)
Huh-7 control	7	10	70
*Huh-7 test	5	5	100
*OPN-A test	5	5	100

Table 5.4 Tumor take rate of naïve and transfectant Huh-7 cell lines in a nude mouse xenograft growth model.

*These tumors represent the Huh-7 test group, which were injected with naïve Huh-7 cells on their left flank and OPN-A cells on their right.

Huh-7 test

Huh-7   OPN-A

5 tumors

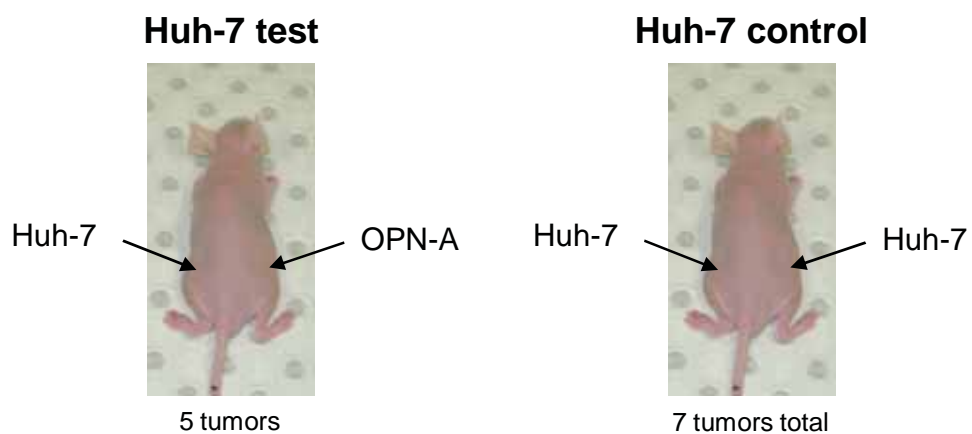**Huh-7 control**

Huh-7   Huh-7

7 tumors total

Figure 5.10 Outline of tumor groups used to ascertain whether OPN secreted from over-expressing tumors affects growth of naïve Huh-7 derived tumors (Huh-7 test group). Both groups contain 5 mice and the diagram above indicates cell lines used for injection into each flank. The number of visible tumors grown for each group is indicated.

Tumors became visible for all groups between days 15 - 18, with no difference in day of tumor appearance noted (Figure 5.11). Tumor growth was monitored daily and graphed until day of culling (Figure 5.12). Growth of OPN-A test tumors was not monitored as these tumors were utilised simply to provide a source of secreted OPN to examine its effect on Huh-7 derived tumor growth. Huh-7 test tumors grew larger and faster than Huh-7 control tumors, however this difference was not significant due to the small number of animals used. A trend however is evident where Huh-7 tumors grown in the presence of OPN-A cells grew faster than those not exposed to OPN. Based on encouraging pilot experiments, further experiments are required using a larger cohort of mice.

5.3 Discussion

5.3.1 OPN expression increases growth rate of Huh-7 derived tumor xenografts

The role of OPN in proliferation of tumorigenic cells remains relatively uncharacterised, especially in relation to HCC. This thesis has previously shown a role for OPN in increased proliferation of cultured hepatoma cells, and suggests that this role is performed in a paracrine manner by OPN secreted from HCC cells (Chapter 4). These results suggest that a similar role may exist for OPN in the proliferation of tumorigenic hepatocytes *in vivo*. A model of subcutaneous Huh-7 xenograft growth in nude Balb/c mice was developed in our laboratory which allowed us to study the effect of OPN expression and secretion on Huh-7 derived tumor growth. Injection of 5×10^6 cells showed 100% tumor take rate and steady tumor growth, resulting in tumors that were highly vascularised and contained cells of human origin undergoing active cell division. This newly developed tumor model provided an excellent model system for the study of OPN's effect on Huh-7 derived tumor growth.
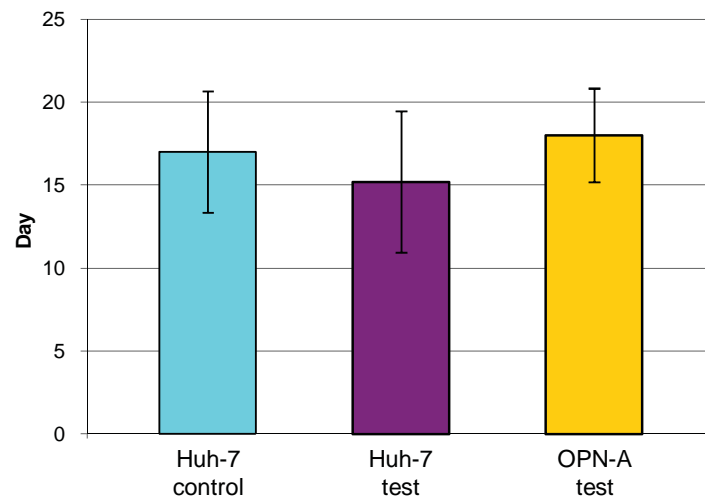
Figure 5.11 Average day of appearance of Huh-7 derived tumors with and without OPN variant overexpression. No significant difference was noted between the test and control tumor groups.
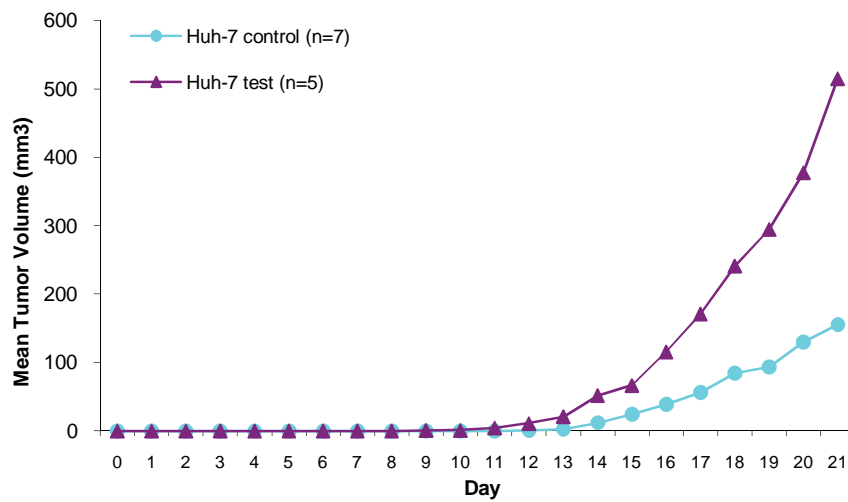
Figure 5.12 Average growth of Huh-7 derived nude mouse xenografts subjected to secreted OPN from OPN-A over-expressing tumors in the same animal, compared to growth of control Huh-7 tumors. Test Huh-7 tumors grew faster and larger than controls, however this increased growth was not significant.

A number of xenograft model systems have previously shown a link between OPN and increased tumor growth, including the use of OPN knock-out cell lines, anti-sense sequences and stable transfectant cell lines (not unlike those used in this study). Tumors derived from OPN stable transfectant murine neuroblastoma (C1300) (Hirama et al., 2003) and human colon (HCT116, SW480) (Irby et al., 2004) and lung (SBC-3) (Cui et al., 2007) cultured carcinoma cells showed significantly increased growth compared to those derived from naïve or mock transfectant cell lines. Silencing of OPN in human breast (MDA-MB-435) (Shevde et al., 2006) and ovarian (HO-8910) (Song, G. et al., 2008) cancer cell lines showed greatly reduced tumor growth compared to naïve cells that expressed low levels of OPN. Blocking of OPN binding to its cell surface receptors by use of RNA aptamers or monoclonal antibodies has also resulted in decreased tumor growth in human breast (MDA-MB-231) (Mi et al., 2009) and lung (SBC-3) (Cui et al., 2007) cancer xenograft models. These studies suggest that increased presence of OPN results in increased tumor growth, and that a lack of OPN through gene silencing or knockout or prevention of OPN-receptor binding retards tumor growth.

Using our newly developed athymic xenograft growth model, tumors derived from Huh-7 cells expressing high levels of OPN-A showed significantly increased tumor growth over those derived from control Huh-7 cells. These OPN-A derived tumors also appeared significantly earlier than control tumors (9 days earlier on average). Huh-7 OPN-B and –C derived tumors appeared at approximately the same time as control Huh-7 tumors, however once established, these tumours had a similar growth rate to that seen for OPN-A expressing tumors. By the day of culling, OPN-B and –C expressing tumors had a tumor volume of approximately three-fold that of control tumors. This dramatically increased growth suggests that, once established, the growth rate of OPN expressing Huh-7 derived tumors increases substantially irrespective of the OPN variant expressed. This suggests similar roles for each of the OPN variants in HCC xenograft

118

growth, which correlates with our previous *in vitro* data that suggests similar roles for the OPN variants in increased Huh-7 cell proliferation (Chapter 4).

Tumor histology revealed the presence of increased tumor vasculature and a higher proportion of Huh-7 cells undergoing mitosis in tumors expressing each of the OPN variants compared to control Huh-7/mock tumors. This observation of increased cell division in OPN expressing tumors correlates with our *in vitro* observations of increased cellular proliferation in hepatoma cells expressing OPN variants. Also observed was the increased vasculature in OPN expressing tumors. This could be due to increased blood supply simply as a consequence of tumor growth or possibly due to the angiogenic potential previously described for OPN (see Section 1.3.6).

The secreted nature of OPN would suggest that it should be detectable in the serum of mice harbouring OPN derived tumours, and thus OPN ELISA was performed on serum and urine from tumor-bearing mice. However, human OPN could not be detected in serum or urine harvested from tumor-bearing nude Balb/c mice (data not shown). This could be due to the Huh-7 derived OPN being rapidly eliminated in the mouse before the time of urine collection, or dilution of secreted OPN from Huh-7 cells into the animal's bloodstream, resulting in OPN levels below the detection limit of the assay. In a previous study, another group also failed to detect human OPN in the serum of mice bearing ANBL-6 human myeloma derived xenografts, even though this cell line has been shown to secrete OPN into conditioned media (Standal et al., 2004). Therefore, from this result the secretion of OPN from Huh-7 cells in the context of a growing tumor could only be assumed in this study.

Nevertheless, we investigated whether OPN acts in a paracrine manner on tumor growth *in vivo* by injecting nude Balb/c mice with Huh-7 cells on one flank and OPN-A expressing Huh-7 cells

on the other. We hypothesised that Huh-7 derived tumors exposed to OPN secreted from a neighbouring tumor would have an increased growth rate compared to Huh-7 tumors not exposed to secreted OPN.

Our results showed that Huh-7 tumors under the potential influence of secreted OPN-A from a distal OPN-expressing tumor grew faster and larger than control Huh-7 tumors, however this result was not significant which is most likely due to the small number of animals used and significant variance in tumor growth. Similar to the previous tumor growth experiment, human OPN could not be detected in murine serum or urine (data not shown). Therefore, whilst our results indicate an increased tumor growth effect for Huh-7 derived tumors grown in the presence of a distal OPN expressing tumor and suggest a role for secreted OPN in increasing tumor growth, we can not conclusively argue that these Huh-7 tumors grew under exposure to secreted OPN. A more sensitive OPN ELISA method may allow for conclusive detection of secreted OPN in murine serum.

In conclusion, the results of this chapter suggest that (i) expression of OPN-A can significantly enhance the growth rate of Huh-7 cells in a tumor xenograft mouse model, (ii) the splice variants OPN-B and C also accelerate Huh-7 growth rates although these tumors are slower in establishing a critical mass, and (iii) OPN bearing tumors show great vascularisation. Collectively we conclude that *in vivo* OPN results in accelerated Huh-7 cell growth which correlates with our *in vitro* data generated in Chapter 4.

5.3.2   Future directions

Our histological analysis of tumours suggest that OPN variants increase the proliferation of Huh-7 cells, however time precluded a more thorough analysis of this proliferation. Future studies should include immunostaining for ki-67 or similar (a marker of proliferating cells) of

Huh-7 derived tumor sections that would allow for enumeration of actively dividing cells. A significant increase in ki-67 positive cells in OPN expressing tumors would suggest increased cellular proliferation due to OPN expression. Concurrently, increased ki-67 staining of Huh-7 tumors exposed to OPN secretion from neighbouring tumors (compared to control Huh-7 tumors) would suggest that secreted OPN increases HCC cell proliferation and therefore tumor growth.

This chapter also suggests that increased tumor growth may be a result of increased vasculature in OPN expressing tumors, although it is difficult to determine if this is a result of OPN expression or a secondary consequence of the need for increased blood supply to the tumor. CD31 staining of Huh-7 derived tumor sections would enable quantitation and comparison of microvessel density. Increased microvessel density in OPN expressing tumors would suggest a role for OPN in neovascularisation of Huh-7 derived tumors which could also contribute to increased tumor growth. OPN is thought to promote angiogenesis through interactions with VEGF (Senger et al., 1996; Shijubo et al., 1999), therefore comparison of tumor VEGF mRNA levels could potentially suggest a pathway through which OPN interactions with VEGF may increase angiogenesis in Huh-7 derived tumors.

The expected action of secreted OPN on Huh-7 derived tumor proliferation in a paracrine manner (as suggested from the results of Chapter 4) could not be confirmed due to the small number of animals used in the second study. However, the trend of increased tumor growth is encouraging and a larger sample size is required if these experiments are to be repeated. OPN secretion from OPN expressing tumors must also be confirmed to ensure that distal Huh-7 tumors are exposed to OPN. This could be achieved by developing a more sensitive ELISA method capable of detecting lower concentrations of human OPN in murine serum.

While we have shown conclusively that OPN can increase Huh-7 cell growth both *in vitro* and *in vivo*, a number of experiments could be performed if time permitted to enhance our observations. Firstly, given the involvement of the CD44-OPN interaction in Huh-7 proliferation it would interesting to produce Huh-7/OPN stable cell lines in a CD44 negative background and determine the phenotype of these cells in *in vivo* tumor growth. Alternatively, tumors could be injected with a lentivirus-expressing shRNA directed to CD44. These experiments would determine the role of CD44 in cellular proliferation. It is also likely that OPN exerts its effect through alteration of the cellular transcriptome. Microarray analysis of tumours representing different OPN variants compared to controls could lead to the identification of pathways responsible for the proliferative effect of OPN.

Given the strong correlation between OPN and metastatic disease described previously (see Section 1.3.6), it would also be interesting to investigate any role for the OPN variants in tumor metastasis in our xenograft growth model. Increased patient plasma OPN has been strongly associated with metastasis of breast (Singhal et al., 1997), gastric (Wu, C. Y. et al., 2007), renal (Ramankulov, Lein, Kristiansen, Meyer et al., 2007), melanoma (Haritoglou et al., 2009), nasopharyngeal (Wong, T. S. et al., 2005), prostate (Ramankulov, Lein, Kristiansen, Loening et al., 2007), and HCC (Zhang et al., 2006) cancers. Increased tumor OPN mRNA levels have also been correlated with HCC metastasis (Pan et al., 2003). A previous study of HCC xenograft growth indicated the presence of metastatic lesions in the lungs of mice subcutaneously injected with a high OPN expressing HCC cell line (HCCLM3) (Sun, B. S. et al., 2008). The number of metastatic lesions was significantly reduced when OPN expression was down-regulated by lentiviral-mediated miRNA interference, strongly suggesting a role for OPN in metastasis of HCC to the lungs. A repeat of our subcutaneous tumor growth experiment using Huh-7 cell lines expressing each of the three OPN variants could be performed whereby organs such as the lungs,

liver, kidney, and brain were harvested for visualisation of possible metastatic lesions. This study would allow for comparison of metastatic activity of the three OPN variants in relation to HCC.

CHAPTER 6: Osteopontin expression in HCV-related liver disease: cellular expression and its potential as a serum biomarker

6.1 Introduction

The search for a reliable diagnostic biomarker of HCC has unearthed many candidates but so far none that can consistently and conclusively diagnose HCC. The most advanced serum biomarker for HCC is α-fetoprotein (AFP), however it suffers from a number of setbacks including a high false positive rate in patients with active hepatitis but no HCC (Johnson, P. J. 2001; Peng et al., 2004) and the fact that up to 30% of HCC patients do not show increased AFP levels above that of healthy patients (Colombo 2001). Other biomarker candidates are currently being investigated, including des-γ-carboxy prothrombin (DCP, aka PIVKA II; currently used as a HCC biomarker exclusively in Japan), glypican-3 (GPC3), golgi protein 73 (GP73), granulin-epithelin precursor (GEP), squamous cell carcinoma antigen (SCCA), and α-1-fucosidase (AFU) (Tangkijvanich et al., 1999; Capurro et al., 2003; Filmus and Capurro 2004; Marrero et al., 2005; Hussein et al., 2008; Lok et al., 2009), however none have shown sufficient sensitivity and specificity for widespread use.

The use of OPN as a potential diagnostic biomarker for a number of cancers has been well studied. Significantly increased serum OPN levels (compared to healthy individuals) have been seen in patients with breast, prostate, lung, ovarian, pancreatic and cervical carcinomas (Table 6.1). Sensitivity and specificity for OPN vary greatly among cancer types (80 - 95% and 66 - 97% respectively) but compare favourably with values observed for established diagnostic tumor biomarkers such as cancer antigen 125 (CA 125; 66.7% and 94.1%) for ovarian cancer (Jacobs et al., 1993), prostate specific antigen (PSA; 34.9% and 63.1%) for prostate cancer (Crawford, E. D. et al., 1999), and AFP (88 - 100% and 40 - 54%) for HCC (Tsai et al., 1990;

Author	Cancer type	Cancer patient OPN (ng/ml)	Control patient OPN (ng/ml)	OPN sensitivity (%)	OPN specificity (%)	Cut off (ng/ml)
Fedarko et al. 2001	Breast	814.0	439.0	95.0	84.5	500.0
	Prostate	653.0	439.0	89.5	69.1	450.0
	Lung	724.0	439.0	95.0	84.5	500.0
Kim et al. 2002	Ovarian	486.5	147.1	80.4	85.4	252.0
Koopman et al. 2004	Pancreatic	482.0	204.0	80.0	97.0	334.0
Cho et al. 2008	Cervical	355.8	100.0	80.0	66.2	113.1

Table 6.1 Previous studies investigating the potential of plasma OPN concentration as a diagnostic biomarker of various cancers. In all studies, control patients were healthy non-diseased individuals.

Fujiyama et al., 1992; Takikawa et al., 1992; Kasahara et al., 1993; Mita et al., 1998; Nakagawa et al., 1999; Ishii et al., 2000). Furthermore, one or both characteristics can be improved when OPN is used in combination with another tumor marker such as SCC antigen for cervical cancer (Cho et al., 2008) or MIA and S-100 β for metastatic uveal melanoma (Barak et al., 2007). The potential use of OPN as a diagnostic biomarker of HCC has been previously investigated, giving high sensitivity (87.1 - 93.5%) and specificity (82.7 - 95%) values when differentiating between HCC and both non-diseased and chronic liver diseased individuals (Kim, J. et al., 2006). This study also compared the effectiveness of OPN as a diagnostic biomarker of HCC to both AFP and DCP using receiver operating characteristics (ROC) analysis, the results of which confirmed OPN as the most accurate diagnostic tool of the three (see Figure 1.18).

The US National Cancer Institute (NCI) defines a tumor biomarker as a substance produced by a tumor or by the host that is detectable in body fluids or tissues and is useful in differentiating neoplastic disease from non-neoplastic disease. Results from this thesis (Section 3.2.4), and those of others, indicate that HCV-related HCC expresses increased levels of OPN mRNA in tumor tissue compared to cognate surrounding tissue and non tumor burdened individuals. Given that OPN is readily secreted into the blood and urine, it fits the description as a potential tumor biomarker of HCC and previous studies would suggest that this may be the case. However, given our data that indicates that OPN expression is increased in progressive HCV-related liver disease (Section 3.2.3), we are also interested to determine if OPN could be used as a biomarker of earlier stages of HCV-related liver disease or to potentially predict which patients may be at risk of developing HCC. Hence, measurement of OPN in the serum of HCV infected individuals may also predict advanced liver disease, not to mention detection of HCC.

The elevated expression of OPN in HCC patients compared to the general population has been well documented, however high serum levels have also been noted in patients with chronic HBV and HCV infection without HCC (Libra et al., 2005; Zhao, L., Li et al., 2008). When tested as a diagnostic tool of HBV-related cirrhosis, OPN had an AUC of 0.928 using ROC analysis (Zhao, L., Li et al., 2008), suggesting it possesses high accuracy as a marker of end-stage HBV-related liver disease prior to development of HCC. To date there is no detailed information regarding OPN expression in HCV-related liver disease, therefore **the aim of this chapter was to investigate OPN expression in serum and tissue samples from non-infected, HCV-infected and HCC-bearing patients to evaluate its potential use as a biomarker of HCV-related liver disease.**

6.2 Results

6.2.1 Expression of OPN in patients with HCV-related liver disease and HCC compared to non-diseased individuals

In order to evaluate and compare serum OPN levels in patients with HCV-related liver disease, and to establish a possible link between OPN expression and degree of liver damage, OPN sandwich ELISA (described elsewhere in this thesis) was performed on our bank of stored serum samples collected from HCV-infected patients, including those with HCC, and OPN serum concentration compared to non-diseased individuals.

6.2.1.1 Sample collection and patient characteristics

Whole blood samples from HCV-positive patients (with and without HCC) were provided by Dr. Hugh Harley (Royal Adelaide Hospital, Adelaide, Australia) as part of their routine clinical management. As soon as possible after collection, samples were centrifuged at 2,000 rpm for 15 minutes and separated serum collected into fresh storage tubes and stored at -20 °C until

required for ELISA testing. Whole blood samples from healthy blood donors, which acted as controls in this study, were donated by the Australian Red Cross Blood Service, Adelaide (n = 49). Serum was harvested from these samples and stored as described above. Patient characteristics for non-diseased individuals (n = 49) and HCV-infected individuals with (n = 6) and without (n = 23) HCC are summarised in Table 6.2.

	Non-diseased (n = 49)	HCV-infected (n = 23)	HCV/HCC (n = 6)
Sex (%)			
Male	21 (43%)	20 (87%)	6 (100%)
Female	28 (57%)	3 (13%)	0 (0%)
Age, yr $\pm$ SD	41.55 $\pm$ 17.68	45.35 $\pm$ 8.8	54.33 $\pm$ 9.87

Table 6.2 Patient characteristics of non-diseased, HCV-infected and HCV-related HCC individuals

6.2.1.2 Serum OPN expression in HCV-related liver disease, including HCC

OPN sandwich ELISA was performed to analyse OPN expression in serum samples outlined in Table 6.2 (Figure 6.1). Serum OPN levels were significantly higher in HCV-infected patients compared to healthy controls (42.00 ng/ml versus 7.29 ng/ml, $p < 0.0001$). This increase in OPN expression was even greater when HCC serum samples were compared to both healthy controls (241.83 ng/ml versus 7.29 ng/ml, $p < 0.0001$) and HCV positive serum samples (241.83 ng/ml versus 42.00 ng/ml, $p < 0.0001$). OPN level was not affected by age or gender in any group (Table 6.3), although gender comparisons could not be made for the HCC group as all patients were male.

Figure 6.1 Serum OPN expression in HCV-infected patients with and without HCC, compared to uninfected individuals. Both groups show increased serum OPN expression compared to uninfected individuals, and those possessing HCC tumors also show increased OPN compared to those that do not have HCC.

	Non-diseased	HCV-infected	HCV/HCC
Mean OPN (ng/ml)	7.29	42.00	241.83
Range	(0-44)	(0-124)	(31-563)
Age (yr)	* p = 0.85	p = 0.20	p = 0.64
< 53	7.91 (0-44)	45.42 (0-124)	227.33 (58-313)
$\geq$ 53	6.12 (0-25)	25.50 (22-31)	256.33 (31-563)
Sex	p = 0.56	p = 0.32	p = n.d.
Male	8.33 (0-34)	39.65 (0-79)	241.83 (31-653)
Female	6.50 (0-44)	57.33 (22-124)	n/a

* p-values were calculated by unpaired student t test. n.d. = not determined. n/a = not applicable.

Table 6.3 Serum OPN levels in non-diseased, HCV-infected and HCV-related HCC patients

Our previous mRNA expression data (Figure 3.8) suggests that OPN mRNA is differentially expressed during different stages of HCV-related liver disease. We therefore investigated whether a similar difference was observed in serum OPN expression by sorting patients according to their stage of liver disease as determined using METAVIR classification (provided by Dr. Andrew Ruszkiewicz, SA Pathology, Adelaide, Australia; Table 6.4). The METAVIR grading system was specifically developed for grading liver disease in patients with Hepatitis C (METAVIR 1994). The system gives a grade indicating the amount of inflammation and a stage representing the amount of fibrosis present. Pathology reports were available for 20 of 23 patients.

Level of fibrosis	METAVIR fibrosis stage	HCV Serum #
No scarring	F = 0	6
Minimal scarring	F = 1	3, 5, 7, 14, 15, 17, 24
Scarring with bridging fibrosis	F = 2/3	1, 2, 4, 9, 11, 12, 21, 22, 23
Advanced fibrosis/cirrhosis	F = 4	8, 16, 18

Table 6.4 Grouping of HCV serum samples based on METAVIR fibrosis stage as assigned by Dr. Andrew Ruszkiewicz (Pathologist, SA Pathology)

OPN ELISA data for HCV-infected serum samples (obtained above) were sorted according to fibrosis level and compared to non-diseased controls and HCC serum samples (Figure 6.2). As previously mentioned, HCV-related HCC sera showed significantly increased OPN compared to healthy controls. When HCV-infected sera samples were divided according to fibrosis stage, those with low (F = 1: 50.86 ng/ml versus 7.29 ng/ml, $p < 0.0001$), medium (F = 2/3: 39.78 ng/ml versus 7.29 ng/ml, $p < 0.0001$) and high (F = 4: 42.00 ng/ml versus 7.29 ng/ml, $p < 0.0001$) fibrosis all showed increased OPN levels compared to non-diseased controls. However, no significant difference in OPN expression was noted between any of the HCV-infected only groups. HCV-related HCC samples showed increased OPN compared to samples with low (241.83 ng/ml versus 86 ng/ml, $p < 0.03$) and medium (241.83 ng/ml versus 39.78 ng/ml, $p < 0.001$) fibrosis but not those with cirrhosis (F = 4). No comparisons could be made to HCV-infected sera with no fibrosis (F = 0) as this group contained only one sample.

As no correlation could be found between serum OPN expression and extent of liver fibrosis, we also stratified HCV serum samples according to their METAVIR activity (A) score in an attempt to correlate serum OPN expression with the degree of liver inflammatory infiltrate, as it has been suggested that OPN is involved in recruiting inflammatory cells during liver disease (Ramaiah
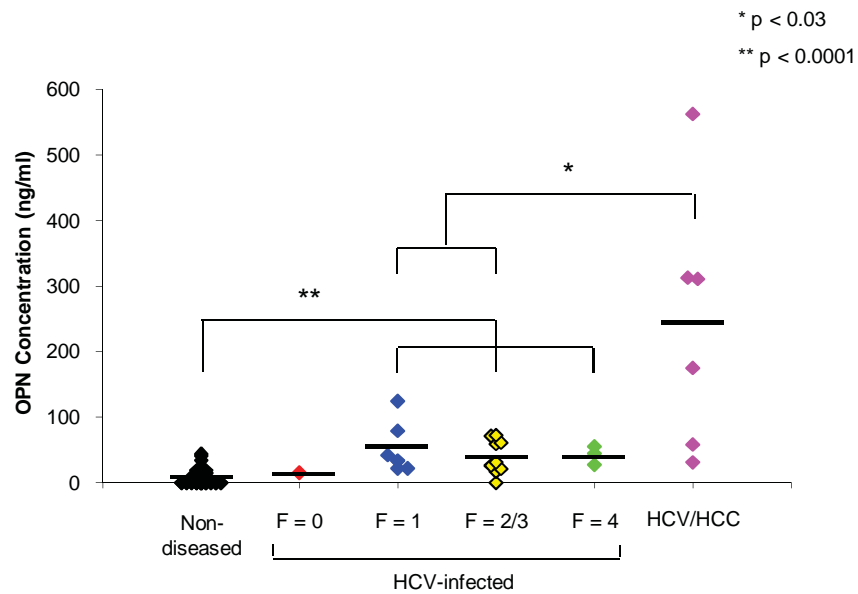
Figure 6.2 Serum OPN expression in HCV-infected patients at varying stages of liver disease. HCV-infected samples with low (F = 1), medium (F = 2/3) and high (F = 4) fibrosis all show increased serum OPN expression compared to healthy controls. HCC samples showed further significant increases in OPN compared to HCV-infected samples with low and medium fibrosis levels, as well as healthy controls (shown previously, see Figure 6.1). No difference was noted between any HCV-infected samples (without HCC) irrespective of fibrosis stage.

and Rittling 2007). OPN serum samples used in Table 6.4 above were grouped according to their A score (Table 6.5). Activity scores were available for 19 of 23 patients.

Degree of liver inflammation (activity)	METAVIR A score	HCV Serum #
No activity	A = 0	none available
Mild activity	A = 1	2, 3, 5, 6, 7, 17, 24
Moderate activity	A = 2	1, 8, 11, 14, 15, 16, 18, 21, 22, 23
Severe activity	A = 3	9, 12

Table 6.5 Grouping of HCV serum samples based on METAVIR activity score as assigned by Dr. Andrew Ruszkiewicz (Pathologist, SA Pathology)

When HCV-infected sera samples were divided according to inflammatory activity, those with mild (A = 1: 42.29 ng/ml versus 7.29 ng/ml, $p < 0.0001$) and moderate (A = 2: 47.00 ng/ml versus 7.29 ng/ml, $p < 0.0001$) inflammation showed increased OPN levels compared to non-diseased controls, and decreased (241.83 ng/ml versus 42.29 ng/ml [$p < 0.03$] and 47.00 ng/ml [$p < 0.001$] respectively) OPN levels compared to HCV-related HCC (Figure 6.3). However, no significant difference in OPN expression was noted between HCV infected livers with varying levels of inflammatory infiltrate. No comparisons could be made to HCV-infected sera with severe inflammation activity (A = 3) as this group contained only two samples.

These results indicate that whilst OPN levels are increased in HCV-positive serum samples prior to HCC development, in our hands there is no significant difference at the fibrosis or inflammation level. While this data strongly suggests that OPN expression is increased in the HCV infected liver, the sample set used was small and clearly a larger cohort of patients are

Figure 6.3 Serum OPN expression in HCV-infected patients with varying degrees of inflammation. HCV-infected samples with mild (A = 1) and moderate (A = 2) inflammation show increased serum OPN expression compared to healthy controls. HCC samples showed further significant increases in OPN compared to HCV-infected samples with mild and moderate activity scores, as well as healthy controls (shown previously, see Figure 6.1). No difference was noted between any HCV-infected samples (without HCC) irrespective of their degree of inflammation.

required to determine if serum OPN is differentially expressed during different stages of fibrosis or inflammation.

6.2.1.3 Cellular OPN expression in HCV-related liver disease, including HCC

Previous results of this thesis have indicated a trend whereby OPN mRNA expression increases with fibrosis stage in HCV-infected livers (see Figure 3.8), and the above results also suggest that HCV-infected patients with liver disease show increased serum OPN. We were therefore interested whether a concurrent increase in OPN mRNA correlated with an increase in OPN protein in the liver. Furthermore, we were also interested to discover which cell types within the HCV-infected liver expressed OPN, given that OPN expression in NHL is restricted to bile duct epithelial cells (Tajiri et al., 2005) while tumor derived OPN is strongly expressed in tumorigenic hepatocytes (Gotoh et al., 2002). Liver biopsy sections representing varying levels of fibrosis were chosen (Table 6.6) from the original patient set used in Section 3.2.3 and stained by IHC for OPN using an OPN-specific antibody.

Level of fibrosis	METAVIR fibrosis stage	HCV Patient #	OPN fold increase (over NHL)
No scarring	F = 0	6	0.75
Minimal scarring	F = 1	29	2.03
Scarring with bridging fibrosis	F = 2/3	4	7.57
Advanced fibrosis/cirrhosis	F = 4	13	23.34
		41	3.62

Table 6.6 Selection of representative HCV liver biopsy sections for OPN IHC based on METAVIR fibrosis stage as assigned by Dr. Andrew Ruszkiewicz (Pathologist, SA Pathology). These sections are matched to the HCV serum samples used in Section 3.2.3

The method used for IHC was the ADVANCE^{TM} HRP (Dako) detection system, a super sensitive system that may detect OPN where other methods have failed in the past. Using this system for OPN detection, NHL showed positive OPN staining in bile duct epithelial cells only (Figure 6.4a) as predicted based on previous reports (see Section 1.3.9.1). The use of an isotype control antibody (rabbit IgG) revealed no positive staining (Figure 6.4b). Similar to NHL, the HCV-infected patient with no fibrosis (F = 0; Patient #6) also showed expression only in bile duct epithelial cells (Figure 6.4c) which is consistent with no increase in OPN mRNA. However, patients with low (F = 1; Patient #29, Figure 6.4e) and medium (F = 2/3; Patient #4, Figure 6.4g) fibrosis showed significant OPN staining in the cytoplasm of hepatocytes. This is consistent with the increased OPN mRNA seen in these patients (2.03 and 7.57 fold over NHL respectively). Interestingly not all hepatocytes stained positive for OPN, with staining localised predominantly in hepatocytes surrounding the central vein. Some positive staining was also noted within cells of the inflammatory infiltrate (Figure 6.4g). Two cirrhotic liver biopsies (F = 4) were chosen for OPN IHC staining. The first showed significantly increased OPN staining in a large proportion of hepatocytes in addition to bile duct epithelial cells (Patient #13, Figure 6.5a). This bile duct expansion (which may occur in CHC) and concurrent staining of hepatocytes correlates well with the 23.34 fold increase in OPN mRNA. Bile duct expansion during HCV-related liver damage has previously been correlated with increasing fibrosis stage and is thought to play a major role in fibrosis progression (Clouston et al., 2005). This study suggested a pathway whereby hepatic progenitor cells are activated in the HCV-infected liver and differentiate into biliary cells, resulting in bile duct expansion which in turn promotes portal fibrosis. The bile duct expansion seen in this cirrhotic biopsy could in some part explain the trend correlating increased liver OPN (both mRNA [Chapter 3] and protein [Chapter 6]) and fibrosis stage. The second biopsy showed a similar hepatocyte expression pattern but at a lower level than that seen in the previous patient (Figure 6.5d). Hepatocyte staining is more evident at the rim of the regenerating hepatocyte

Figure 6.4 Representative IHC staining showing increasing OPN protein expression in HCV-infected livers as the degree of liver fibrosis increases. NHL **(a)** shows positive OPN staining only in bile duct epithelial cells (**1**→); this has been described previously in the literature. HCV-infected liver with no fibrosis and similar OPN mRNA expression relative to NHL (Section 3.5.3.3) **(c)** also shows OPN expression only in bile duct epithelial cells. HCV-infected liver with low levels of fibrosis and a 2-fold increase in OPN mRNA **(e)** shows strong OPN staining in the cytoplasm of a small proportion of hepatocytes (**2**→). This trend continues with HCV-infected liver with medium fibrosis and a 7-fold in increase in OPN mRNA **(g)**, which also shows strong cytoplasmic OPN staining in a higher proportion of hepatocytes. The isotype control antibody reveals a very low level of background staining for all sections (**b, d, f, h**).
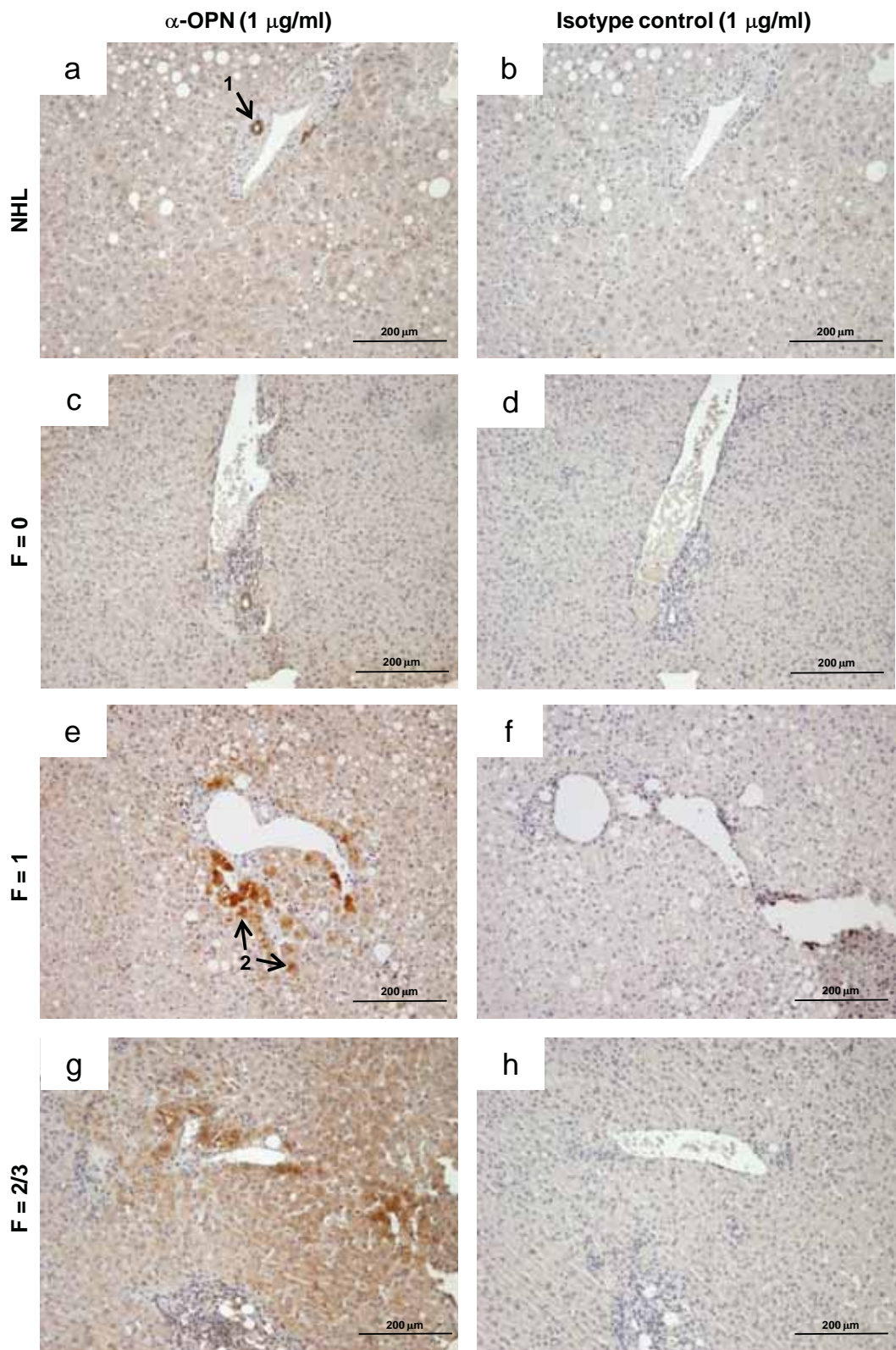
α-OPN (1 μg/ml) Isotype control (1 μg/ml)

Figure 6.5 Representative IHC staining showing increased OPN protein expression in HCV-infected livers with cirrhosis, the final stage of HCV-related liver disease prior to HCC development. Patient 1 **(a, b, c)** showed a 23.34-fold increase in OPN mRNA (see Figure 3.8) which is confirmed by IHC staining. Strong OPN staining is seen in bile duct epithelial cells **(1→)** and the cytoplasm of hepatocytes **(2→)**. This OPN staining is seen in greater detail in higher magnification **(c)** of the outlined area as indicated in **(a)**. Patient 2 **(d, e, f)** showed a 3.62-fold increase in OPN mRNA which is also confirmed by IHC staining. Positive OPN staining is observed again in bile duct epithelial cells and the cytoplasm of hepatocytes, however the level of staining is much lower than that seen in the previous section. Also, OPN seems to be more concentrated in hepatocytes around the rim of the nodule of regenerating hepatocytes **(3→).** The isotype control antibody **(b, e)** reveals a very low level of background staining for both tumors.

α-OPN (1 μg/ml)

Isotype control (1 μg/ml)
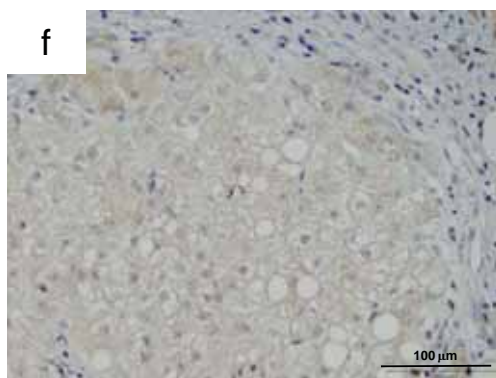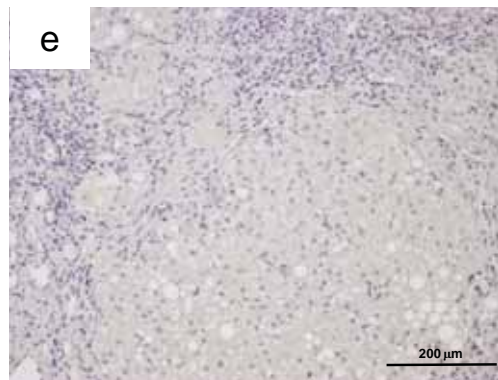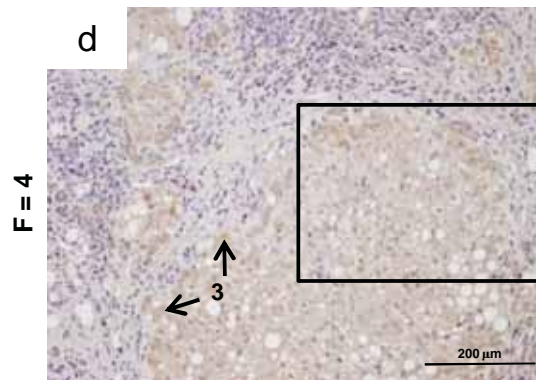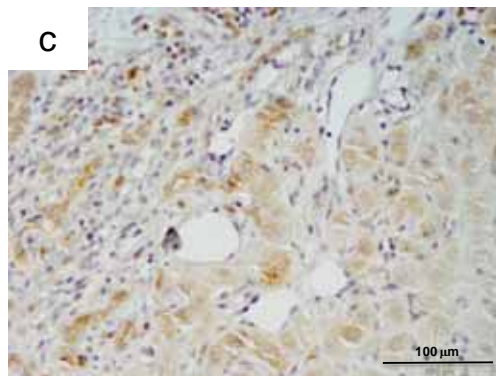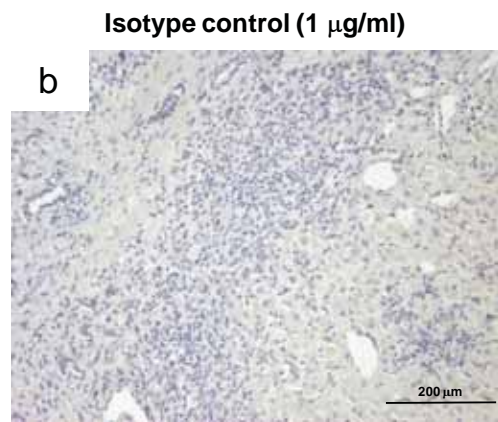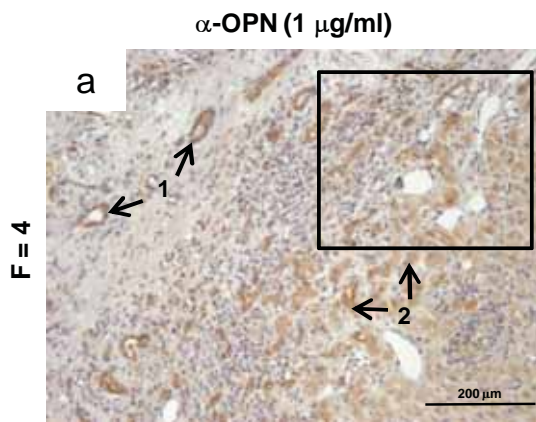
nodule. The isotype control antibody showed a very low level of background staining for all tissue sections (Figure 6.4b, d, f, h and Figure 6.5b and e). Therefore, OPN IHC staining shows increased OPN protein expression as the degree of liver disease increases, which is consistent with increases in OPN mRNA shown previously in this thesis. This demonstrates for the first time in chronic hepatitis C that there is a shift of OPN expression from the bile duct epithelial cells to the hepatocyte, similar to that noted in HCC and raises the question as to the role of hepatocyte derived OPN in HCC development.

6.2.2   Expression of OPN in patients with HBV and alcohol related liver disease and HCC

Our studies suggest that OPN may be a biomarker of HCV-related liver disease and HCC, however it remains to be determined if this increase in OPN is specific to CHC. Previous published reports suggest that OPN expression is not specific to HCV-related liver disease (Kim, J. et al., 2006; Zhao, L., Li et al., 2008). To clarify and extend these observations we investigated OPN expression in serum from HBV-infected individuals, including those with HBV-related HCC provided by Prof. Ed Gane (Auckland Hospital, New Zealand), and from patients with alcohol induced HCC provided by Dr. Tin Nguyen (Royal Prince Alfred Hospital, Melbourne, Australia). Firstly, serum samples from patients with confirmed HCC induced by HBV infection (n = 17) or ethanol consumption (EtOH/HCC; n = 22) were analysed for OPN expression by sandwich ELISA and compared to that previously observed for patients with no known liver disease and HCV-related HCC (Section 6.2.1.2). Patient characteristics for all sets of patients are outlined in Table 6.7.

	Non-diseased (n = 49)	HBV/HCC (n = 17)	EtOH/HCC (n = 22)	HCV/HCC (n = 23)
Sex (%)				
Male	21 (43%)	12 (71%)	21 (95%)	6 (100%)
Female	28 (57%)	4 (11%)	1 (5%)	0 (0%)
Age, yr $\pm$ SD	41.55 $\pm$ 17.68	n/avail	56.14 $\pm$ 9.31	54.33 $\pm$ 9.87

n/avail = patient characteristics (including sex and/or age) were not available to us.

Table 6.7 Patient characteristics of non-diseased individuals and those with HBV, ethanol and HCV-related HCC

Similar to HCV-HCC there was a significant increase in serum OPN for HBV-related HCC (187.42 ng/ml versus 7.29 ng/ml, $p < 0.0001$) and ethanol-induced HCC (48.78 ng/ml versus 7.29 ng/ml, $p < 0.0001$; Figure 6.6) compared to non-diseased individuals. OPN level was not affected by age or gender in any group (Table 6.8), although gender comparisons could not be made for the ethanol-induced and HCV-related HCC groups as all patients were male (except for a single female EtOH/HCC patient).
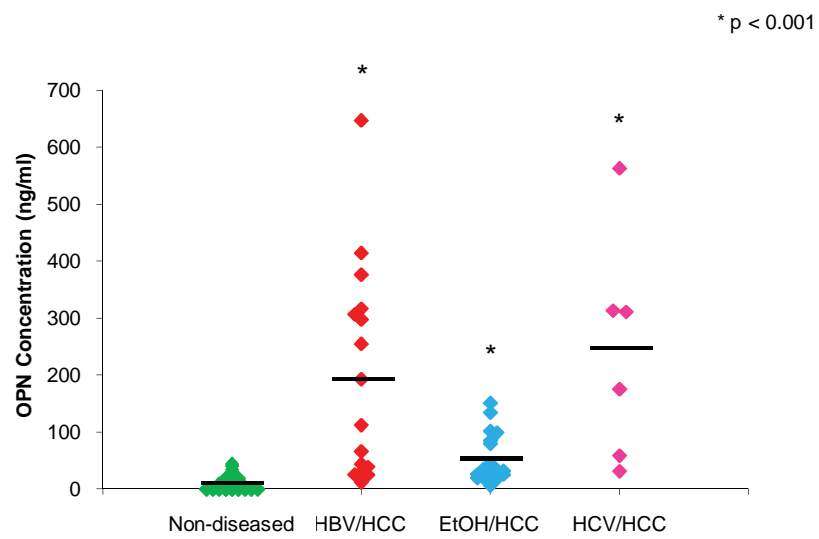
Figure 6.6 Serum OPN levels of patients with HBV, ethanol (EtOH) and HCV-induced HCC are all significantly higher than non-diseased individuals. * p < 0.001 compared to non-diseased individuals.

	Non-diseased	HBV/HCC	EtOH/HCC	HCV/HCC
Mean OPN (ng/ml)	7.29	187.42	48.78	241.83
Range	(0-44)	(12-647)	(6-151)	(31-563)
Age (yr) < 53 ≥ 53	* p = 0.85 7.91 (0-44) 6.12 (0-25)	n/avail	p = 0.031 72.00 (26-151) 33.83 (6-99)	p = 0.64 227.33 (58-313) 256.33 (31-563)
Sex Male Female	p = 0.56 8.33 (0-34) 6.50 (0-44)	p = 0.34 169.25 (25-376) 274.50 (12-647)	p = n.d. 48.78 (6-151) 19 (19-19)	p = n.d. 241.83 (31-653) n/a

* p-values were calculated by unpaired student t test. n.d. = not determined. n/a = not applicable. n/avail = patient characteristics (including sex and/or age) were not available to us.

Table 6.8 Serum OPN levels in non-diseased individuals and HBV-related, ethanol (EtOH)-induced and HCV-related HCC patients

Interestingly a significant difference was observed in OPN levels between ethanol-induced HCC and both virally-induced HBV/HCC ($p < 0.002$) and HCV/HCC ($p = 0.0001$). The reasons for this are unclear and may reflect the different etiology of the two groups of HCC. It would be interesting for future studies to examine the histology of these HCCs and to determine the distribution of OPN by IHC staining.

To extend these observations and to confirm published reports (Zhao, L., Li et al., 2008) we then investigated whether OPN could be used as a biomarker of earlier stages of damage in HBV-induced liver disease. Serum OPN levels from HBV positive patients without HCC were compared to healthy individuals and HBV-induced HCC patients (used in the experiment described above). The HCC negative HBV patients were split into two groups based on the presence ($n = 36$) or absence ($n = 44$) of cirrhosis. Patient characteristics are outlined in Table 6.9, with no difference in gender distribution or age observed between any group.

	Non-diseased (n = 49)	Non-cirrhotic HBV (n = 44)	Cirrhotic HBV (n = 36)	HBV/HCC (n = 17)
Sex (%)				
Male	21 (43%)	n/avail	23 (64%)	12 (71%)
Female	28 (57%)		13 (36%)	4 (11%)
Age, yr ± SD	41.55 ± 17.68	n/avail	49.06 ± 10.88	n/avail

n/avail = patient characteristics (including sex and/or age) were not available to us.

Table 6.9 Patient characteristics of non-diseased, HBV-infected (with and without cirrhosis) and HBV-related HCC patients

Samples for all patients were exposed to OPN sandwich ELISA to determine their individual levels of OPN expression. OPN was significantly increased in HBV-HCC serum samples as expected. Furthermore, both non-cirrhotic (58.61 ng/ml versus 7.29 ng/ml, $p < 0.0001$) and cirrhotic (73.02 ng/ml versus 7.29 ng/ml, $p < 0.01$) HBV-infected patients also showed increased serum OPN expression compared to healthy individuals (Figure 6.7). However, no difference in OPN expression was observed between cirrhotic and non-cirrhotic HBV-infected sera. OPN expression was further significantly increased in HBV-related HCC over both non-cirrhotic (187.42 ng/ml versus 58.61 ng/ml, $p < 0.0001$) and cirrhotic (187.42 ng/ml versus 73.02 ng/ml, $p < 0.0001$) HBV-infected patients. OPN level was not affected by age or gender in any group (Table 6.10). These results confirm the published results of Zhao *et al.*, (2008).

Figure 6.7 Serum OPN expression in HBV-infected patients with varying levels of liver disease, compared to uninfected individuals. All groups show increased serum OPN expression compared to uninfected individuals, and those possessing HCC also show increased OPN compared to those that do not have HCC tumors. No difference was noted between HBV-infected patients with and without cirrhosis. NS = not statistically significant.

	Non-diseased	Non-cirrhotic HBV	Cirrhotic HBV	HBV/HCC
Mean OPN (ng/ml)	7.29	58.61	73.02	187.42
Range	(0-44)	(0-345)	(0-1042)	(12-647)
Age (yr)	* p = 0.85	n/avail	p = 0.24	n/avail
< 53	7.91 (0-44)		102.32 (0-1042)	
≥ 53	6.12 (0-25)		27.07 (0-201)	
Sex	p = 0.56	n/avail	p = 0.58	p = 0.34
Male	8.33 (0-34)		86.22 (0-1042)	169.25 (25-376)
Female	6.50 (0-44)		49.77 (0-435)	274.50 (12-647)

* p-values were calculated by unpaired student t test. n/avail = patient characteristics (including sex and/or age) were not available to us.

Table 6.10 Serum OPN levels in non-diseased, HBV-infected (with and without cirrhosis) and HBV-related HCC patients

6.3 Discussion

6.3.1 Serum and liver OPN levels are increased in HCV-related liver disease including HCC

Elevated OPN expression in HCC (from a number of causes) has been widely reported and was confirmed in this chapter for HCV, HBV and ethanol related HCC. Tumor biomarkers currently used to detect and screen for HCC include AFP and DCP, however both suffer from low specificity and diagnostic accuracy as described elsewhere in this thesis (see Sections 1.2.5.2 and 6.1). A number of alternative markers are currently under intense investigation, however there remains a clear need for a specific and sensitive high-throughput serum biomarker to detect HCC and early stages of liver disease (which may aid in the assessment of risk towards long-term development of HCC). During the course of this thesis we have shown an increase in OPN mRNA expression in both HCV-related HCC and HCV-related liver disease. This suggests a

potential role for OPN as a diagnostic biomarker for not only HCC but for pre-cancerous stages of HCV-related liver disease. The identification of such a precancerous biomarker of HCC would significantly enhance the early detection of HCC lesions through screening programs leading to improved patient outcomes and reduced cost to health care systems. This chapter investigated this potential in greater detail.

The results of this chapter showed a significant increase in serum OPN concentration in HCV-infected patients both with and without HCC compared to healthy individuals, regardless of gender or age. While this was expected for those with HCC the finding of increased OPN levels in the serum of patients with HCV-related liver disease was novel at the time of this study. Consistent with our findings, a recent publication has shown that that OPN expression was increased in HCV-related liver disease and correlated with inflammation and degree of fibrosis (Huang et al., 2010). Our observations are consistent with a number of *in vitro* cell culture and *in vivo* mouse models that suggest a role for OPN in liver fibrosis and inflammation. OPN has been associated with the fibrotic process through activation of hepatic stellate cells and production of collagen (Marra 1999; Lee, S. H. et al., 2004; Cao and Liu 2006). Furthermore, it has also been shown to facilitate macrophage and neutrophil infiltration into the liver and upregulate IL-12 and IL-18 expression, all-important components of the inflammatory response (Sato, T. et al., 2005; Banerjee et al., 2006; Ramaiah and Rittling 2007; Banerjee et al., 2009). Unlike the study of Huang and colleagues we noted no such correlation which is most likely a reflection of the small number of patient samples examined. Nevertheless, we did find increases in OPN expression in HCV-related liver disease and future studies are required using a larger cohort of patient samples to further explore the relationship between OPN and liver inflammation and fibrosis.

In normal liver tissue OPN is expressed in bile duct epithelial cells while in HCC OPN is expressed predominantly in tumorigenic hepatocytes, often at the leading edge of cancerous nodules. Thus there is a significant shift in OPN expression between the bile duct epithelial cells in the normal liver to HCC-derived cells in primary liver cancer. However, the cells responsible for OPN expression between the normal liver and a cancerous one have not been described and were a focus of this chapter. Determining the cells types responsible for OPN expression in HCV-related liver disease could shed light onto its function in liver disease and its potential role in development of HCC. As expected, liver histology revealed positive IHC OPN staining predominantly in the bile duct epithelial cells of normal liver and in a HCV-infected liver with no fibrosis. However, in HCV infected livers with fibrosis (METAVIR F = 2 - 4) significant OPN expression was observed in hepatocytes, particularly those around the central vein and at the rim of the regenerating hepatocyte nodule in fibrosis grade 4. Interestingly, OPN expression was not expressed in all hepatocytes suggesting differential regulation of OPN expression. Increased OPN expression at sites of hepatocyte regeneration has been noted previously in fulminant hepatic failure (Arai et al., 2006). Considering that staining was predominantly concentrated at areas of high regeneration, it could be argued that only cells undergoing active proliferation express high levels of OPN. However, in these studies it was not determined if OPN had a role in cellular proliferation or was expressed as a consequence of the damaged/stressed hepatocytes. The findings of this thesis may well explain that OPN may play a role in hepatocyte proliferation under disease conditions. The results presented in this thesis are significant in that they show for the first time expression of OPN in hepatocytes in the HCV infected liver or any other diseased liver for that matter. Thus it is not difficult to hypothesise that as liver disease progresses there is a shift in the cell type and level of expression of OPN. This raises the question as to the role of OPN in the development of HCC and suggests a potential involvement of OPN in hepatocyte transformation in the HCV-infected liver.

Whilst the results of this chapter clearly indicate that patients with varying levels of HCV-related liver disease show increased serum and liver OPN levels, further investigation reveals that this phenomenon is not specific to HCV-infected patients. Analysis of HBV-infected serum also showed a significant increase in OPN expression in both cirrhotic and non-cirrhotic individuals without HCC, however no significant difference was noted between these groups. HBV and HCV are the two leading indicators for cirrhosis and HCC and while these viruses are unrelated (HBV is a DNA virus that can integrate while HCV is a ssRNA virus), viral infection of the liver results in similar processes of host inflammatory responses directed against virally-infected hepatocytes. Therefore, it is logical that increases in OPN seen in HCV-infected patients would also be visualised in HBV-infected patients. This also suggests that it is not the virus itself that induces OPN expression but is as a result of host factors induced in the viral infected liver.

It is interesting to note that in our study we also observed an increase in OPN expression in alcohol induced HCC. However, OPN was increased to significantly lower levels that that seen in either HBV or HCV-related HCC. The pathogenesis of viral hepatitis-induced liver damage is markedly different to that caused by alcoholic liver disease and may explain this increase in OPN. Viral infection with HBV or HCV results in large-scale inflammation and hepatocyte death and regeneration as a result of the host inflammatory response attempting to rid the liver of virally-infected cells, whereas excessive alcohol consumption blocks the normal consumption of proteins, fats and carbohydrates leading to oxidative stress, hypoxia, steatosis and cellular necrosis. OPN's widely reported role in inflammation could result in a higher requirement for OPN during the virally-induced inflammatory response and thus explain the observed result. Host factors may also play an increased role in virally-induced liver disease due to the heightened immune response against virally-infected hepatocytes.

In conclusion, the results of this chapter indicate that (i) serum OPN is increased in pre-cancerous stages of HCV-related liver disease, however (ii) this phenomenon is also apparent in individuals with HBV-related liver disease and (iii) it does not discriminate between varying stages of liver disease prior to HCC development in the small cohort of patients examined, however larger studies are required. This chapter also confirmed increased OPN expression in HCV, HBV and ethanol related HCC, but did note a difference in OPN levels between ethanol- and virally-induced HCC.

6.3.2   Future directions

Whilst the results of this chapter report OPN increases in HCV- and HBV-related liver disease, the significance of this data suffers from small sample sets. Increasing the number of samples for each experiment and ensuring equal representation of the different stages of liver disease would solidify the observed results and potentially uncover a correlation between OPN expression and degree of liver disease for HBV and/or HCV-related liver disease as has been noted by others (Zhao, L., Li et al., 2008; Huang et al., 2010). Given that OPN is selectively expressed in hepatocytes it would be interesting to investigate global gene expression in these cells or those close by (as OPN acts in both an autocrine and paracrine manner); this could be performed using laser capture dissection and comparing gene expression patterns with hepatocytes distal to those expressing OPN using microarray technology. Given we have shown that OPN increases hepatocyte proliferation, we hypothesise that these OPN expressing cells may show gene expression patterns consistent with cellular proliferation. Future experiments should also include OPN knock-out mice (Liaw et al., 1998) in which liver regeneration studies (partial hepatectomy) and models of fibrosis (carbon tetrachloride: CCL4) could be performed to determine the role of OPN in these processes.

The results of this pilot study suggest a potential for OPN as a diagnostic biomarker of not only HCC but also earlier stages of both HBV and HCV-related liver disease, and may also have merit as a predictive marker for future HCC development in HCV-infected patients. However, further research is required to fully investigate the diagnostic potential of OPN. Calculation of the specificity and sensitivity of OPN as a diagnostic marker of HCC and its diagnostic efficiency can be calculated using a receiver operating characteristics (ROC) curve and compared to other HCC serum markers such as AFP and DCP. Previous calculations for OPN covering a range of cancers have shown similar rates to established cancer biomarkers as described previously (see Section 6.1). The study by Zhao *et al.,* (2008) showed that OPN could be used to accurately predict cirrhosis in HBV-infected patients with a ROC score of 0.928. A number of groups have successfully increased diagnostic accuracy when combining two or more serum markers; this approach could be used for OPN.

CHAPTER 7: Concluding Remarks

The overall aim of this thesis was to investigate the expression and function of OPN and its variants in the context of HCV-related liver disease and HCC. While OPN is significantly expressed in a high proportion of HCCs we know little regarding its expression during the early stages of liver disease that precedes HCC development. Furthermore, OPN is expressed as three variants and the relative roles for these OPN forms are unknown. In Chapter 3 we showed for the first time that OPN expression is increased in the liver at the mRNA level from patients with chronic hepatitis C. Although our patient cohort was small a trend towards an increase in expression of OPN mRNA with increasing complexity of liver disease was noted although not significant. This strongly suggests that OPN is not solely expressed in HCC and its expression in the early stages of liver disease may play a role in development of HCC. We also showed for the first time that OPN is expressed as three variants (OPN-A, -B and –C) in both HCC derived cell lines, tumor tissue and in HCV-related liver disease. The role of these alternative variants is unknown and forms the basis of our studies in Chapter 4. Attempts to devise a quantitative assay to determine the relative abundance of specific OPN isoforms was technically challenging and presented numerous difficulties. While we were able to amplify OPN isoforms individually using a quantitative RT-PCR approach, cross-priming precluded accurate quantitation and further work is required to optimise such an assay. If indeed specific OPN variants are associated with a specific tumor phenotype or outcome such as patient survival or metastatic potential then a quantitative OPN isoform assay could be useful in patient management. We showed expression of all three variants in HCC cell lines and in patient samples (HCC, HCV-related liver disease) although OPN-A was the dominant species with varying expression of OPN-B and –C. Interestingly, cell lines of murine origin and HCC that developed in mice transgenic for HCV protein expression expressed OPN-A only. This suggests that perhaps in the context of tumor development OPN-A has a primary role in establishing an environment suitable for tumor growth

and OPN-B and –C have secondary function. Further studies are required to investigate this observation.

While a wide variety of potential functions have been described for full-length OPN (OPN-A) the alternative variants OPN-B and OPN-C remain relatively uncharacterised, particularly in relation to cellular proliferation. The role of OPN in cellular proliferation is a controversial topic, with conflicting reports suggesting that OPN can increase proliferation of some tumor-derived cells but not others. To date there is a paucity of information on the role of OPN and variants in HCC proliferation. The results of Chapter 4 in which we cloned all OPN forms and derived stable Huh-7 OPN-expressing clones showed that all three variants were able to significantly increase proliferation of cultured hepatoma cell lines in an autocrine and paracrine manner. This observation is novel and we hypothesised that this growth-promoting effect may occur through the interaction of secreted OPN with one of its major cell-surface receptors CD44. Through the use of a CD44 negative cell line (Hep3B) and down-regulating CD44 mRNA and protein expression with siRNA oligonucleotides we showed that CD44 expression is essential for OPN-mediated cellular proliferation. Furthermore, by blocking of the binding sites of both OPN and CD44 via antibodies we also showed that the interaction between OPN and CD44 is essential in this process. By showing this similar effect for all three OPN variants, we have also determined that the lack of exons experienced by both OPN-B and OPN-C does not affect their tertiary structure or their ability to bind to the cell surface receptor CD44. This is the first report of OPN inducing cellular proliferation through an interaction with CD44 and now raises the question as to the cellular signals involved in driving this proliferative effect following the OPN/CD44 interaction.

In Chapter 5 we extended our observations noted in Chapter 4 and showed that, like *in vitro*, Huh-7 cells expressing each of the OPN variants significantly accelerated cell growth in a nude mouse xenograft growth model. Interestingly, cells expressing OPN-A established tumors more rapidly than cells expressing OPN-B or –C which suggests that all OPN isoforms are promoters of cellular proliferation, although OPN-A may be more efficient at establishing tumors. This observation is consistent with our murine OPN data in which we could not detect OPN-B or-C in either cell lines or HCC derived from mice transgenic for HCV genome expression. Collectively our *in vitro* and *in vivo* data strongly suggest that all OPN variants play a significant role in HCC cell derived cellular proliferation through a CD44 dependent signaling mechanism. Work in Chapter 6 extended our focus to the clinical application of OPN expression and showed that serum OPN expression was not only elevated in HCC but also in the serum of patients with chronic hepatitis C. This increase in expression was not restricted to HCV-related disease as OPN was also elevated in HBV and ethanol related liver disease and HCC. As OPN fits the criteria for a potential clinical biomarker this raises the question as to the usefulness of measuring serum OPN to predict stages of HCV-related liver disease. We clearly showed that OPN expression was elevated in HCV-related liver disease although this did not correlate with the METAVIR classification of liver disease, however our patient cohort was relatively small and investigation of a larger sample set is required. We also showed for the first time that OPN is expressed in hepatocytes in the HCV-infected liver which represents a shift in expression from bile duct epithelial cells in the non diseased liver.

In conclusion, at the molecular level we have shown that OPN is expressed as three variants that all have the ability to enhance cellular proliferation through interaction with the cellular receptor CD44. Thus it is not inconceivable that blocking the OPN/CD44 interaction may be an attractive targeted therapeutic strategy to limit the growth of HCC and further studies are required to

investigate this possibility. In addition, at the clinical level we showed that OPN expression is elevated in HCV-related liver disease which is often a precursor environment for the development of HCC. The challenge will now be to determine if those patients with elevated OPN are more susceptible to HCC development; this will require long-term monitoring of a longitudinal cohort of HCV-infected individuals. Furthermore, the work of this thesis suggests that monitoring of HCV-infected individuals with moderate to advanced liver disease may be useful to predict or detect which patients are at risk of developing HCC, although investigation of a larger cohort of patients is required to determine if this is a real possibility.